THE SOLAR WIND AND ITS ANGULAR MOMENTUM

Thesis by

Edmund J. Weber

In Partial Fulfillment of the Requirements

For the Degree of

Doctor of Philosophy

California Institute of Technology

Pasadena, California

1967

(Submitted May 19, 1967)

ACKNOWLEDGMENTS

The writer wishes to express his sincerest thanks to his advisor, Professor Leverett Davis, Jr., for his helpful suggestions and encouragement throughout the course of this investigation.

Thanks are also due to Professor R.F. Christy who gave suggestions and advice on the problems of numerical integration and to Dr. G.L. Siscoe for many discussions of this work as a whole. The author is also grateful for the financial support during portions of this investigation from a Woodrow Wilson Fellowship and from grant No. NsG 426 of the National Aeronautics and Space Administration.

ABSTRACT

A steady-state model is developed for the solar wind in the equatorial plane. Included in the equation of motion are forces due to gravity, viscosity, pressure gradients and magnetic fields. The electrical conductivity of this plasma is taken to be infinite. Since it is impossible to determine the qualitative features of the solar wind motion from a study of the complete set of equations, a simplified model is treated at first. This model has an isotropic pressure, no viscosity and an energy supply characterized by a polytrope law. It is found that the solution of the radial motion must pass through three critical points, whose significance is explained in terms of the characteristic velocities with which small amplitude disturbances propagate. Similarly, the solution of the azimuthal motion has to pass through the radial Alfvénic critical point where the radial Alfvénic Mach number equals unity. The conditions at this point together with the solution of the radial motion then determines uniquely the values of the azimuthal velocity and of the magnetic field everywhere, in particular at the surface of the sun. A numerical solution is obtained for typical parameters. The solution indicates that the magnetic field produces only a modest tendency toward corotation of the solar wind, azimuthal velocities of the order of 1 km sec^{-1} at 1 a.u. being typical, but that the magnetic stresses apply a torque to the sun equal to that required to produce effective corotation out to the radial Alfvénic critical point. For typical solar wind values this will occur between

15 and 50 solar radii out, which implies a substantial loss in the angular momentum of the sun.

The polytrope model does not represent a very real model of the energy supply to the solar wind. To obtain information on the energy transport in the inner part of the solar system a solar wind model is developed in which the density distribution between the photosphere and 10 $r_\odot$ is determined from observations and where between 10 $r_\odot$ and 1 a.u. heat is supplied by thermal conduction only. With this model the amount of heating due to waves in the solar corona can be determined.

Since the azimuthal motion does not influence the radial motion appreciably, the stability of the azimuthal motion is investigated on the assumption that the radial solution is a given function of distance. It is shown that under these conditions disturbances travel along the characteristics and that for such disturbances the model is stable. Using the same assumption about the radial velocity, the effect of viscosity and anisotropy in the pressure on the azimuthal motion is investigated. The results indicate that the total torque on the sun is slightly less than that obtained from the non-viscous model, but that the torque on the solar wind due to these additional forces results in an azimuthal velocity at 1 a.u. which is approximately 5 km sec^{-1}.

TABLE OF CONTENTS

I. AN INTRODUCTION TO THE SOLAR WIND

I.1 Particles in Interplanetary Space

Interplanetary space, the region between the sun and the planets had for a long time been tacitly treated as a vacuum, void and empty, except for comets, asteroids, light, and cosmic rays. In reality it is filled with a large number of moving particles which make up what is referred to as the interplanetary medium. These particles have a great range in energy and with few exceptions have originated at the sun. As they move outward from the sun, these particles determine the over-all properties of interplanetary space.

Thus the inner boundary of this region, if one may speak of this as a boundary at all, is the top of the sun's atmosphere, indeed a very poorly defined surface. The transition between the sun's corona and interplanetary space is so gradual that one can easily consider the interplanetary space as the sun's uppermost atmospheric region, which then, of course, implies that all the planets move in the atmosphere of the sun.

The large extent of the solar atmosphere is due to the fact that the solar corona has a temperature of a few million degrees. The gravitational field of the sun cannot contain this hot gas and thus the corona expands continuously. In the corona with its high temperature, all elements are ionized and because of the low probability of recombination, gases which move out from the sun will in general remain ionized to a distance of at least a few astronomical units. The continuous, steady stream of ionized gas particles which is emitted

from the sun constitutes an electrically neutral plasma, which is highly conducting electrically. It is therefore strongly influenced by and coupled to the magnetic fields which are present, which in turn are affected by the motion of the plasma. To this process the name "solar wind" has been given (Parker, 1958).

In addition to this steady "boiling off" of particles from the quiet sun, there occur transient and localized emission of particles. These originate from active regions on the sun, where violent processes throw particles off which will travel with very much higher velocities than the solar wind. These particles may reach the earth in a few minutes to hours, whereas the solar wind requires a few days for this journey.

As the solar wind with the magnetic field embedded in it flows away from the sun it will eventually come to a region, where the momentum flux of this outflowing gas and the interstellar cosmic ray plus magnetic pressure become comparable to each other. In this region, the solar wind will be slowed down, and a shock wave will be produced. This region may be considered as the outer boundary of interplanetary space.

I.2 Early Work and Experimental Observations

The earliest known suggestions of a close connection between auroras, geomagnetic storms and other related phenomena and a possibly existing solar corpuscular radiation were made around the turn of the century (FitzGerald, 1892, 1900; Lodge, 1900). They were generally ignored or even argued against very strongly (Kelvin, 1892). It was the close parallelism between the fluorescence produced by cathode rays

in a tube and the aurora in the atmosphere that had triggered the suggestion of the existence of a solar corpuscular radiation which could excite the atoms in the upper atmosphere and thus produce the aurora. Very detailed observations of auroras and geomagnetic activity and related laboratory experiments on magnetized spheres were performed by Birkeland (1908, 1913) in the period from 1897 until 1903. It was largely due to his work and later work by Stormer (1955) and Chapman (1918, 1919) that the idea of the existence of particle streams from the sun began to gain acceptance. Some thirty years later, Chapman and Ferraro (1931) derived theoretical models that explained how such effects as the sudden commencement and the initial phase of a geomagnetic storm could be accounted for by localized streams of particles thrown off the sun. About the same time, the anti-correlation of the galactic cosmic-ray intensity with the solar activity was discovered by Forbush (1938). The observations of acceleration of molecular ions in the tail of type I comets by Wurm (1943) led Biermann (1951) to suggest that the emission of particles from the sun was a continuous process.

With the availability of deep space probes a new era has begun in this field. It has now become possible to determine in some detail the properties of the interplanetary medium in the vicinity of the earth. Mariners II and IV even permitted us to obtain certain data for the region between Venus and Earth and Earth and Mars, respectively. These and other space probes have provided much needed data on particle velocity, density, and magnetic fields outside the earth's magnetosphere. Neugebauer and Snyder (1966), Wolfe, Silva, and Meyers (1966) and others have observed a steady stream of particles near 1 a.u., which is

supersonic. At the same time measurements of the magnetic field have been made and were reported by Davis, Smith, Coleman, and Sonnett (1966) and Ness, Scearce and Seek (1964). Within the last year satellites have been launched with still more sophisticated measuring devices, with which more detailed studies of the solar wind properties can be made. During the part of the solar cycle that has been explored, the typical solar wind near 1 a.u. may be described as having a velocity which is nearly radial and has a magnitude between 300 km sec^{-1} and 700 km sec^{-1} with occasional excursions to perhaps 275 km sec^{-1}, and, when the sun is active, to at least 800 km sec^{-1}. The observed particle densities are usually of the order of 2 to 10 ions cm^{-3} even though 3-hour density averages on Mariner II have ranged from as low as 0.4 ions cm^{-3} to values as high as 80 ions cm^{-3}. The solar wind proton temperature varies between 3×10^4 and 9×10^5 ^oK with an average value of approximately 1.8×10^5 ^oK. The average interplanetary magnetic field near 1 a.u. has a magnitude which fluctuates from approximately 2 to 8γ and the field vector lies mainly in the equatorial plane. A typical set of average solar wind values is represented by a radial velocity of 400 km sec^{-1}, a density of 5 ions cm^{-3}, a temperature of 2×10^5 ^oK and a magnetic field of 5γ.

I.3 Theoretical Investigations and Scope of Present Work

Biermann's (1951) suggestion that the sun emitted corpuscular radiation continuously was for some time largely ignored or rejected. Parker (1958) revived the idea by demonstrating that the solar corona would not be in hydrostatic equilibrium and thus had to expand

continuously. Later work of Parker (1963,1965) dealt with more general properties of a radially expanding plasma. Many other investigators have discussed various properties of the solar wind, but until very recently all models treated were restricted to plasmas with purely radial flow only, in which magnetic forces had been neglected. Parker (1963) has discussed some of the general properties which the magnetic field in the solar wind should have.

The present work treats the motion of a plasma which has an azimuthal as well as a radial velocity and which carries embedded in it a magnetic field. From the solution of the azimuthal equation of motion we obtain the value of the torque which the solar wind exerts on the sun in the equatorial region. In addition we will show that from a solution of the solar wind equation together with a knowledge of the coronal density we are able to deduce the amount and distribution of energy which has to be deposited in the corona to drive the solar wind. Finally, we will discuss some of the effects which an anisotropic pressure tensor and viscosity may have on the azimuthal motion of the solar wind in the presence of a magnetic field.

Very recently, papers by Brandt (1966), Pneuman (1966), Modisette (1967) and Weber and Davis (1967) have begun an exploration of the problem treated here.

II. THE SOLAR WIND MODEL

II.1 Basic Postulates and Assumptions

In this model we will use the magneto-hydrodynamic equations of a perfectly conducting fluid to describe the behavior and properties of the solar wind. For this to be true, randomizing processes have to exist and operate in the region of interest. If Coulomb collisions were the only such process acting in the solar wind, the hydrodynamic approximation would be inappropriate as soon as we get out from the sun more than a few solar radii. The success with which models, using the hydrodynamic equations, have predicted the general behavior and the over-all properties of the solar wind all the way out to the orbit of Mars can be considered the best proof that there exist other randomizing processes in interplanetary space besides Coulomb collisions. Such processes may be scattering from local field irregularities and local instabilities which tend to make the velocity distributions isotropic. There may still be many other mechanisms which are not yet known. All indications which we have at the present time seem to support the assumption that the hydrodynamic or magneto-hydrodynamic equations are a reasonably accurate means of describing the properties of the solar wind.

In our model the sun is assumed to have a general magnetic field that depends only on latitude. The local irregularities in the field, the polarity reversals and wind velocity fluctuations of the sector structure, and the waves superimposed on the smooth field in interplanetary space are all unessential in treating the basic behavior of

the solar wind. The average magnetic field in the equatorial plane can have no substantial component normal to this plane as has been shown by Davis (1966). Accordingly, we will examine primarily a steady state model with complete axial symmetry and mirror symmetry about the equatorial plane in which the field is combed out by the solar wind. There will be a flux return at other latitudes which we do not need to consider if we concentrate our attention on the solar wind in the equatorial plane only. Thus in spherical polar coordinates r, the distance from the center of the sun, is the only independent variable, there being no φ dependence. We assume further the plasma in the solar wind is made up of pure hydrogen. The presence of helium ions in the solar wind will give only relatively slight complications which do not affect the results significantly.

For simplicity the functional dependence of variables on r will not be indicated. All variables with a subscript $(\ )_\odot$ refer to values for the sun, those with subscript $(\ )_o$ to values at an arbitrary reference level, those with $(\ )_e$ to values at the earth's orbit, i.e., at 1 a.u., and those with subscripts $(\ )_c$, $(\ )_a$, and $(\ )_f$ to values at the three critical points which will be derived in the solution and which will be explained in the next section. In all our work we will further assume that in the steady-state solar wind the velocities and magnetic fields as well as their derivatives are continuous, smooth functions of position, i.e., no shocks exist anywhere.

II.2 Solar Wind Equations

In the equatorial plane we may describe the velocity of the solar wind by

$$\underset{\sim}{v} = u\, \underset{\sim}{e}_r + v_\varphi\, \underset{\sim}{e}_\varphi \qquad \text{(II.2.1)}$$

where r, θ, φ are the usual spherical polar coordinates in an inertial frame whose polar axis is the sun's axis of rotation. In the steady state, conservation of mass requires that

$$\rho u r^2 = \text{constant} \qquad \text{(II.2.2)}$$

where ρ is the mass density in gm cm^{-3}. The magnetic field is given in a similar way by

$$\underset{\sim}{B} = B_r\, \underset{\sim}{e}_r + B_\varphi\, \underset{\sim}{e}_\varphi \qquad \text{(II.2.3)}$$

But from Maxwell's equation we know that div B = 0 and hence

$$r^2 B_r = \text{constant} = r_o^2 B_{ro} \qquad \text{(II.2.4)}$$

The solar wind is a perfect conductor and thus the electric field in an inertial frame $\underset{\sim}{E}$ is given by

$$\underset{\sim}{E} = -\frac{\underset{\sim}{v} \times \underset{\sim}{B}}{c} \qquad \text{(II.2.5)}$$

in Gaussian units. In a steady state we obtain furthermore from Maxwell's equations

$$c(\nabla \times \underset{\sim}{E})_\varphi = \frac{1}{r}\frac{d}{dr}\left[r(uB_\varphi - v_\varphi B_r)\right] = 0 \qquad \text{(II.2.6)}$$

But in a perfectly conducting fluid, $\underset{\sim}{v}$ is parallel to $\underset{\sim}{B}$ in a frame that corotates with the sun. This allows us to evaluate the constant which we obtain from the integration of Eq. (II.2.6) and thus

$$r(uB_\varphi - v_\varphi B_r) = \text{constant} = -\Omega r^2 B_r \qquad \text{(II.2.7)}$$

where Ω is the angular velocity of the roots of the lines of force in the sun.

This model has φ symmetry and we may obtain the equation of motion in the φ-direction in the following way. Let us consider a ring of fluid bounded by surfaces at r, r + Δr and $\theta = 90^{o} + \Delta\theta/2$. This ring has volume $2\pi r^{2}\Delta r\ \Delta\theta$ which moves outward with a radial velocity u. As this annulus moves out, the change in the angular momentum of the fluid enclosed in this volume must equal the net torque on it, i.e.,

$$\frac{d\ell}{dt} = \oint_{S} \underset{\sim}{n}\cdot(\underset{\approx}{T} \times \underset{\sim}{r})\ da \qquad \text{(II.2.8)}$$

Here ℓ is the angular momentum in the volume, $\underset{\sim}{n}$ is a unit vector directed outward from the surface and da is a surface element, and $\underset{\approx}{T}$ is the total stress tensor. The integral is to be evaluated over the total surface S enclosing the volume of the fluid. As the annulus moves outward its thickness Δr is given by

$$\Delta r = u\ \Delta t \qquad \text{(II.2.9)}$$

where Δt is a constant time interval. The angular momentum of the fluid in the annulus is given by

$$\ell = 2\pi r^{3}\rho\ v_{\varphi}\ \Delta r\ \Delta\theta \qquad \text{(II.2.10)}$$

The cross product under the integral in Eq. (II.2.8) is defined by

$$(\underset{\approx}{T} \times \underset{\sim}{r})_{\lambda\mu} = T_{\lambda\sigma}\ \eta^{\alpha\sigma\tau}\ r_{\tau}\ \frac{g_{\alpha\mu}}{\sqrt{g}}$$

where $\eta^{\mu\sigma\tau}$ is the completely asymmetrical tensor and g is the determinant of the metric tensor. The metric tensor in turn is given by

$$g_{ij} = \begin{pmatrix} 1 & 0 & 0 \\ 0 & r^2 & 0 \\ 0 & 0 & r^2 \sin^2\theta \end{pmatrix}$$

The surface integral on the right-hand side of Eq. (II.2.8) can now be evaluated quite readily to give

$$T_{r\varphi}(r + \Delta r)2\pi(r + \Delta r)^3\Delta\theta - T_{r\varphi}(r)2\pi r^3\Delta\theta = 2\pi\Delta\theta\Delta r \frac{d}{dr}(r^3 T_{r\varphi}) \qquad \text{(II.2.11)}$$

This is the only contribution to the integral since we restrict our discussion to the equatorial plane, and with the assumption that v_φ depends only as sin θ on the polar angle θ, the $T_{\theta\varphi}$ component is identically zero. Using Eqs. (II.2.9), (II.2.10), and (II.2.11) we can now evaluate Eqs. (II.2.8). In a steady state this yields

$$2\pi\ \Delta\theta\ \Delta t\ u \frac{d}{dr}(u\rho r^2\ rv_\varphi) = 2\pi\ \Delta\theta\ \Delta t\ u \frac{d}{dr}(r^3 T_{r\varphi}) \qquad \text{(II.2.12)}$$

which may be integrated immediately to give

$$\rho u r^2\ rv_\varphi = r^3 T_{r\varphi} + K\ \rho u r^2 \qquad \text{(II.2.13)}$$

where $K\ \rho u r^2$ is a constant of integration. The total stress tensor $\underset{\approx}{T}$ is made up of the Maxwell stress tensor $\underset{\approx}{M}$ and the mechanical stress tensor $\underset{\approx}{\sigma}$, which is just the negative of the pressure tensor $\underset{\approx}{p}$ plus the viscous stress tensor $\underset{\approx}{\sigma}^o$. Thus we may write for the $r\varphi$ component of $\underset{\approx}{T}$

$$T_{r\varphi} = M_{r\varphi} + \sigma_{r\varphi} = \frac{1}{4\pi} B_r\ B_\varphi - p_{r\varphi} + \sigma_{r\varphi}^{\ o} \qquad \text{(II.2.14)}$$

We will discuss how one may calculate $\sigma_{r\varphi}$ and $p_{r\varphi}$ in Section IV and in Appendix A.

To describe completely the motion of the solar wind we need an equation to express the conservation of linear momentum in the solar wind. The forces acting on the plasma in the radial direction are those due to the gravitational attraction of the sun, the gradient of the scalar pressure in the radial direction, the magnetic forces, the centrifugal force due to the azimuthal motion of the wind and all those additional forces which are caused by the terms in the mechanical stress tensor. Thus we can take as the steady state radial momentum equation

$$\rho u \frac{du}{dr} = - \rho \frac{GM_\odot}{r^2} - \frac{dp}{dr} + \frac{1}{c} (\underset{\sim}{J} \times \underset{\sim}{B})_r + \rho \frac{v_\varphi^2}{r} + \frac{1}{r^3} \frac{d}{dr} (r^3 \sigma^o_{rr} - r^3 p_{rr}) \tag{II.2.15}$$

where G is the universal gravitational constant, $M_\odot$ is the mass of the sun and $\underset{\sim}{J}$ is the current density. Appendix A gives a derivation which indicates how the last term is calculated. But from Maxwell's equation we know that

$$\underset{\sim}{J} = \frac{c}{4\pi} \underset{\sim}{\nabla} \times \underset{\sim}{B} \tag{II.2.16}$$

and thus the magnetic force in the radial direction may be expressed as

$$\frac{1}{c} (\underset{\sim}{J} \times \underset{\sim}{B})_r = - \frac{1}{4\pi r} B_\varphi \frac{d}{dr} (rB_\varphi) \tag{II.2.17}$$

As the equation of state of the solar wind plasma we may use the ideal gas law. Since in a fully ionized gas of pure hydrogen the total number of particles is $2\rho/m$, where m is the mass of the hydrogen atom, the equation of state is

$$p = \frac{2kT}{m}\rho \qquad \text{(II.2.18)}$$

where T is the temperature of the gas (assumed equal for ions and electrons), and k is Boltzmann's constant. In order to determine a connection between the temperature and the density, we need an energy equation. As the solar corona expands and forms the solar wind, the total energy flux has to be a constant, since there are no sources or sinks in interplanetary space. The total energy flux per steradian, F, is given by

$$F = r^2\rho u\left(\frac{1}{2}u^2 + \frac{1}{2}v_\varphi^2 - \frac{GM_\odot}{r} + \frac{5kT}{m}\right) + r^2\left(\frac{B_\varphi^2}{4\pi}u - \frac{B_\varphi B_r}{4\pi}v_\varphi\right)$$

$$- ur^2\sigma_{rr}^o - \kappa r^2\frac{dT}{dr} + r^2S(r) \qquad \text{(II.2.19)}$$

where κ is the thermal conductivity of the plasma which is proportional to $T^{5/2}$(Chapman and Cowling, 1952; Chapman, 1954), S(r) is a source function whose physical significance we shall discuss in more detail later.

On the right-hand side of Eq. (II.2.19) the terms in the first bracket represent the energy convected out by the solar wind itself in the form of kinetic and potential energies and in its enthalpy. The terms in the second bracket represent the Poynting energy flux, while the third and fourth terms are the energy flux associated with the viscous stress tensor (Scarf and Noble, 1964) and the heat conduction, respectively. To explain the physical significance of the last term it is best to consider the conditions near the surface of the sun in more detail. It is observed that the temperature of the solar plasma

increases as we go outward from the visible surface and the photosphere to the chromosphere and the corona, with the latter reaching a temperature of a few million degrees. The corona looses energy constantly by heat conduction and due to the solar wind. This energy has to be supplied to the corona in some way, otherwise it would cool off very rapidly. Alfvén (1947), Biermann (1948), Schwarzschild (1948), Parker (1960) and Osterbrock (1961) have presented physical explanations of this phenomenon. Today it is generally assumed that the corona is principally heated by the dissipation of hydromagnetic waves, which in turn were generated from internal gravity waves and the dissipation of shock waves in the chromosphere. This heating by hydromagnetic wave dissipation is not necessarily confined to the lower solar corona, but may extend for a significant distance out from the sun and thus supply energy to the solar wind directly. This additional energy flux from the sun will be represented by the function S. Since we have at the present time very little quantitative information about this heating mechanism and the dissipation of hydromagnetic waves, we do not know anything about the form of this function S(r). In Section III.6 of this thesis we will discuss how a knowledge of the density function in the vicinity of the sun will enable us to determine the amount of energy deposition required in the solar corona and in the solar wind, and thus, in turn, will allow us to obtain information about this function.

The total energy flux as given by the right-hand side of Eq. (II.2.19) is a constant. Thus we have basically four equations, namely (II.2.7), (II.2.13), (II.2.15), and (II.2.19) in four unknowns:

u, v_φ, B_φ, T. All other variables may be expressed in terms of these four by use of the other equations. As they stand these equations form a set of non-linear, second order differential equations which cannot be solved analytically. Even numerical solutions are very difficult, if not impossible, for the following reasons. First and foremost, the function S is unknown and we have at the present time neither a theory which would predict its form and properties, nor experimental results from which it could be determined directly. One could overcome this difficulty by arguing that this function S is identically zero and that the energy transported by heat conduction is sufficient to drive the solar wind. This may be justified beyond approximately $2r_\odot$, but it is certainly not correct in the region between the sun's surface and $2r_\odot$. But even if one considers a case for which $S = 0$, one will find that it is still extremely difficult, if not impossible,to obtain numerical results for the complete set of equations. The reason for this is that the equations are very sensitive and that there exist critical points which govern the behavior of the solution. A more elaborate and detailed discussion of this fact will be given in the next section. Furthermore, while we wish to understand the general behavior of the solar wind in as much detail as possible, we wish in this discussion mainly to investigate the angular motion of the solar wind and the effect it has on the angular momentum of the sun. Therefore, we shall discuss in the next sections two slightly simpler models of the solar wind, which will nevertheless give us a great deal of insight into the behavior and a good understanding of the properties of the solar wind.

III. MODELS OF THE SOLAR WIND WITH AN ISOTROPIC PRESSURE TENSOR

III.1 General Discussion

The major difficulty which we encounter in trying to solve the set of Eqs. (II.2.7), (II.2.13), (II.2.15), and (II.2.19) which describe the solar wind is the presence of the traceless mechanical stress tensor $\underset{\approx}{\sigma}$. Models of a purely radially moving solar wind in which this tensor has been replaced simply by the ordinary viscous stress tensor as given by Landau and Lifshitz (1959) have been investigated by Scarf and Noble (1965), and Whang, Liu and Chang (1966). Parker (1965) and Meyer and Schmidt (1966) have commented on these solutions and the latter authors have argued that the presence of the magnetic field in the interplanetary space should change the form of the viscosity term drastically. Similarly Pneuman (1966) has investigated the purely azimuthal motion of the solar wind using again the viscous stress tensor as given by Landau and Lifschitz. Since the stress tensor $\underset{\approx}{\sigma}$ and especially its $\sigma_{r\varphi}$ component will be significantly altered by the presence of the magnetic field and the anisotropy which is thus introduced in space, we do not feel that the results obtained neglecting the presence of the magnetic field in a discussion of the azimuthal motion of the solar wind will predict properly the behavior of the solar wind. On the other hand, if we neglect all effects on the motion due to any anisotropy in the pressure, and if we furthermore consider a non-viscous model of the solar wind, we shall have a model which, although not complete, is simple enough that we can solve it readily. Furthermore,

solution will be complete enough to give a sound understanding of

the azimuthal motion of the solar wind, the extent to which there is effective corotation, and the rate of loss of angular momentum from the sun. In addition, we will be able to calculate the effect which the azimuthal motion of the solar wind and the presence of the magnetic field have on the radial motion itself.

In the general framework of non-viscous, isotropic pressure models we shall discuss and solve in detail a model in which S(r) is assumed to behave in such a way that T and ρ are connected by a polytrope law. This model will then be used to obtain the desired results for the azimuthal wind velocity and the torque exerted by the solar wind on the sun. Secondly, we shall discuss a model which uses the complete energy equation (II.2.19), except that σ^{o}_{rr} and p_{rr} are set equal to zero, thus obtaining S(r) from the observed run of density near the sun, from the assumption that S is zero beyond a given distance from the sun and from suitable boundary conditions at 1 a.u.

III.2 Polytrope Model of the Solar Wind

Since we have no information about the nature and distribution of sources of energy in the solar wind, we will not try to determine the temperature from the energy equation (II.2.19). Instead we will make the approximation that is usual when the sources are poorly known and use the polytrope law

$$p = p_o\left(\frac{\rho}{\rho_0}\right)^{\gamma} = p_a\left(\frac{\rho}{\rho_a}\right)^{\gamma} \qquad \text{(III.2.1)}$$

where γ is the polytropic index.

If there is a large amount of heating in the neighborhood of

the sun, then we would expect γ to have a value close to 1 in this region. On the other hand, very far away from the sun we expect that there is no substantial heating of the solar wind due to waves, etc., and if the temperature drops sufficiently fast, there will also be practically no heating due to thermal conductivity. Thus γ should approach the adiabatic value of 5/3 as r becomes large. It is hence clear that γ is really not constant, but is a slowly varying function of r. Nevertheless, let us, for simplicity, treat the case in which γ is a constant and then later indicate the effect of making γ a slowly varying function. Using the polytrope approximation to the energy equation, we may immediately rewrite the radial momentum equation (II.2.15):

$$\rho u \frac{du}{dr} = - \rho \frac{GM_\odot}{r^2} - \gamma \frac{p_a}{\rho_a} \left(\frac{\rho}{\rho_a}\right)^{\gamma-1} \frac{d\rho}{dr} - \frac{B_\varphi}{4\pi r} \frac{d}{dr} (rB_\varphi) + \rho \frac{v_\varphi^2}{r} \tag{III.2.2}$$

where use has been made of Eq. (II.2.17). Since we assume $\sigma_{ij} = 0$ we can evaluate Eq. (II.2.13) using only the magnetic terms of Eq. (II.2.14) for the stress tensor and obtain

$$r v_\varphi - r \frac{B_r B_\varphi}{4\pi\rho u} = L \tag{III.2.3}$$

where we have used L instead of K for the constant of integration. This gives us now two equations relating v_φ and B_φ, namely (II.2.7) and (III.2.3) which may be solved for either one of these variables as a function of u and r only. First, it is convenient to introduce a new variable, M_A, which we call the radial Alfvénic Mach number and which is defined by

$$M_A^2 = \frac{4\pi\rho u^2}{B_r^2} \qquad \text{(III.2.4)}$$

Now, solving for the azimuthal velocity, we obtain

$$v_\varphi = \Omega r \frac{(M_A^2 L r^{-2} \Omega^{-1} - 1)}{(M_A^2 - 1)} \qquad \text{(III.2.5)}$$

The radial Alfvénic Mach number M_A is much smaller than 1 near the surface of the sun, but at 1 a.u. M_A is approximately 10. Thus there exists a point between the sun and the earth where $M_A = 1$; let the radius and radial velocity at this point be called r_a and u_a, respectively. This point will be called the Alfvénic critical point. The denominator of the above expression will go to zero at this point and the angular velocity would become singular unless the numerator vanishes identically at the same point. Thus the condition that v_φ must remain finite at the Alfvénic critical point requires that the magnetic field must arrange itself so that the constant L has the value

$$L = \Omega r_a^2 \qquad \text{(III.2.6)}$$

But from Eqs. (II.2.2), (II.2.4), and (III.2.4), we see that $M_A^2/(ur^2)$ is a constant which may be evaluated at the Alfvénic critical point to give

$$M_A^2 = \frac{ur^2}{u_a r_a^2} = \frac{\rho_a}{\rho} \qquad \text{(III.2.7)}$$

This reduces Eq. (III.2.5) to

$$v_\varphi = \frac{\Omega r}{u_a} \frac{(u_a - u)}{1 - M_A^2} \qquad \text{(III.2.8)}$$

The azimuthal magnetic field is thus given by

$$B_\varphi = - B_r \frac{\Omega r}{u_a} \frac{r_a^2 - r^2}{r_a^2 (1 - M_A^2)} \qquad \text{(III.2.9)}$$

The asymptotic behavior of these functions, v_φ and B_φ can now be obtained. For $r \gg r_a$, the radial velocity, u, in the usual solutions is almost a constant, u_∞ and thus $M_A \propto r$ and both v_φ and B_φ vary as 1/r. For $r \ll r_a$, where $u \ll u_a$, Eq. (III.2.9) gives us for the azimuthal field

$$B_\varphi = - B_r \frac{\Omega r}{u_a} \left[1 - \frac{r^2}{r_a^2}\left(1 - \frac{u}{u_a}\right) + \text{---}\right] \qquad \text{(III.2.10)}$$

whereas

$$v_\varphi = \Omega r \left[1 - \frac{u}{u_a}\left(1 - \frac{r^2}{r_a^2}\right) + \text{---}\right] \qquad \text{(III.2.11)}$$

Near the surface of the sun most of the angular momentum loss is due to the torque exerted by the magnetic fields. As we go farther away from the sun, the azimuthal fluid velocity increases and the magnetic stress decreases until at large distances their relative contributions to the total angular momentum loss are $[1 - (u_a/u_\infty)]$ and u_a/u_∞, respectively. An important feature of the solution which is worth noting is that the constant L is not determined by the values of B_φ and v_φ at the sun. Instead, L is determined from conditions at the Alfvénic critical point and this fixes B_φ. At the surface of the sun, where the density becomes very large and the radial velocity approaches zero, we can see from Eq. (III.2.10) that the φ component of the magnetic field does not go to zero as has been assumed by many

investigators, but approaches the value $- B_r \frac{\Omega r}{u_a} (1 - r^2/r_a^2)$. Having thus obtained expressions for v_φ and B_φ which are functions of u and r only, we can use these expressions as well as the mass conservation equation (II.2.2) to rewrite the momentum equation (III.2.2) as a first-order, non-linear differential equation. After some algebraic manipulation we obtain

$$\frac{du}{dr} = \frac{u}{r} \frac{N(u,r)}{D(u,r)} \qquad \text{(III.2.12)}$$

where the numerator function is given by

$$N(u,r) = \left(2\gamma \frac{p_a}{\rho_a} M_A^{-2(\gamma-1)} - \frac{GM_\odot}{r} \right) (M_A^2 - 1)^3 + \Omega^2 r^2 \left(\frac{u}{u_a} - 1 \right) \left[M_A^2 \left(\frac{u}{u_a} - 3 \right) + \frac{u}{u_a} + 1 \right] \qquad \text{(III.2.13)}$$

and the denominator is given by

$$D(u,r) = \left(u^2 - \gamma \frac{p_a}{\rho_a} M_A^{-2(\gamma-1)} \right) (M_A^2 - 1)^3 - \Omega^2 M_A^2 (r_a^2 - r^2)/r^2 \qquad \text{(III.2.14)}$$

It will be noted immediately that the Alfvénic critical point $r = r_a$ *is also a critical point of the radial equation. As we shall see below* this differential equation possesses two additional critical points. For a polytrope model with its simple relationship between p, T, and S, the energy equation is the integral of the radial momentum equation. Thus for this model we obtain for F, the total energy flux per steradian

$$F = \rho u r^2 \left\{ \frac{u^2}{2} + \frac{\gamma}{\gamma - 1} \frac{p_a}{\rho_a} M_A^{-2(\gamma-1)} - \frac{GM_\odot}{r} + \frac{\Omega^2 r_a^4}{2r^2} \left[1 + \frac{(2M_A^2 - 1)(r^2 - r_a^2)^2}{r_a^4 (M_A^2 - 1)^2} \right] \right\} \qquad \text{(III.2.15)}$$

Since we have written F as a function of u and r only, the fourth term in the above equation represents the sum of the magnetic and rotational energies. Since we use a polytropic law, the second term is the sum of the enthalpy and the energy transported by thermal conduction, and waves as described by S(r).

Equation (III.2.15) supplies us with an algebraic equation relating u and r. Before we proceed to solve this equation, it is interesting to investigate the behavior of the solution in general.

III.3 Properties and Topology of the Radial Solution

If we consider the region close to the surface of the sun, we can obtain two asymptotic forms for the radial velocity u which are given by

$$u = u_o r^{(3-2\gamma)/(\gamma-1)}[1 + a_1 r - a_2 r^3 + \cdots] \qquad \text{(III.3.1)}$$

and

$$u = b_o r^{-1/2}[1 + b_1 r - b_2 r^{(5-3\gamma)/2} + \cdots] \qquad \text{(III.3.2)}$$

Equation (III.3.1) shows clearly that there is no solution in which u approaches zero for small r when $\gamma > 3/2$. As r tends to zero, the density increases as $r^{-1/(\gamma-1)}$ for the case of (III.3.1) and as $r^{-3/2}$ for the case of (III.3.2). The constants a_0, a_1, a_2, b_0, b_1, b_2 depend on the initial conditions and the parameters entering Eq. (III.2.15). If the solutions are required to run through the critical points, these constants depend on the properties there. The asymptotic behaviors at large distances are given by

$$u_\alpha = \alpha_0 \left[1 + \alpha_1 \frac{1}{r^{2(\gamma-1)}} + \alpha_2 \frac{1}{r} + \alpha_3 \frac{1}{r^2} + \text{---}\right] \qquad \text{(III.3.3)}$$

and

$$u_\beta = \beta_0 r^{-2} \left[1 - \frac{1}{r^2}(\beta_1 - \beta_2/r) + \text{---}\right] \qquad \text{(III.3.4)}$$

where again the values of the α's and β's are determined in the same way as the constants of Eqs. (III.3.1) and (III.3.2). It is of interest to determine in particular the asymptotic behavior of those solutions which pass through the critical points. If the constants are evaluated for these solutions we find that two branches behave like u_α and two like u_β. If we call these solutions $u_{\alpha 1}$, $u_{\alpha 2}$, $u_{\beta 1}$, and $u_{\beta 2}$, then we find that $u_{\alpha 1}$ gives the behavior of a supersonic, super-Alfvénic wind at infinity, whereas $u_{\alpha 2}$ will remain super-Alfvénic, but becomes subsonic again after passing through the critical points. If $u_{\alpha 1}$ has a velocity at infinity of 425 km sec^{-1} then the value for $u_{\alpha 2}$ will be approximately 9 km sec^{-1}. For both $u_{\alpha 1}$ and $u_{\alpha 2}$ the pressure tends to zero as r becomes very large. The remaining two solutions $u_{\beta 1}$ and $u_{\beta 2}$ yield non-zero pressures at infinity.

The topology of the solution is shown in Figure III.3.1 which appears to show two critical points only, a standard "X"-type singularity at $r = r_c$ and a much higher order singularity at $r = r_a$. Actually, as shown by Figure III.3.2, which is an enlargement of a small area around r_a of Figure III.3.1, two singularities nearly coincide, one being a higher order singularity at $r = r_a$ and the other a simple "X"-type singularity slightly further out at $r = r_f$.

If one performs an expansion around $r = r_c$ and $r = r_f$, one finds

that both of these points are standard "X"-type singular points. The same procedure does not work around $r = r_a$. If one sets

$$r = r_a(1 + \epsilon) \tag{III.3.5}$$

$$u = u_a(1 + \delta) \tag{III.3.6}$$

then Eq. (II.3.4) becomes to lowest order

$$\frac{d\delta}{d\epsilon} = \frac{\delta}{\epsilon} \tag{III.3.7}$$

which can be solved immediately to give

$$\delta = m\epsilon \tag{III.3.8}$$

If one uses an expansion in which the next higher term is retained we obtain a fourth order equation in m. If calculations are made it is found that two roots are real and two are complex. The real roots have different signs and give the directions with which solutions $u_{\alpha 1}$ and $u_{\beta 2}$ pass through the radial Alfvénic critical point. If a more general form for δ is used such as

$$\delta = k\ \epsilon^n \tag{III.3.9}$$

one finds that the only permissible value of n is 1.

The four branches $u_{\alpha 1}$, $u_{\alpha 2}$, $u_{\beta 1}$, and $u_{\beta 2}$ are indicated also on Figures III.3.1 and III.3.2. In order to have a solution for which u goes to zero for small r and has a value close to the observed one at 1 a.u. the solution has to pass through all three critical points. This means that the detailed behavior of the solution will depend very largely on these critical points. As usual, all these singularities are found

Figure III.3.1

Family of solutions of Eq. (III.2.14) for a given γ and r_a. The solutions passing through the critical points are designated as u_{α_1} and u_{α_2} (with zero pressure at infinity) and u_{β_1} and u_{β_2} (with non-zero pressure at infinity).

Figure III.3.2

Enlargement of Figure III.3.1 about the critical point $r/r_a = 1$.

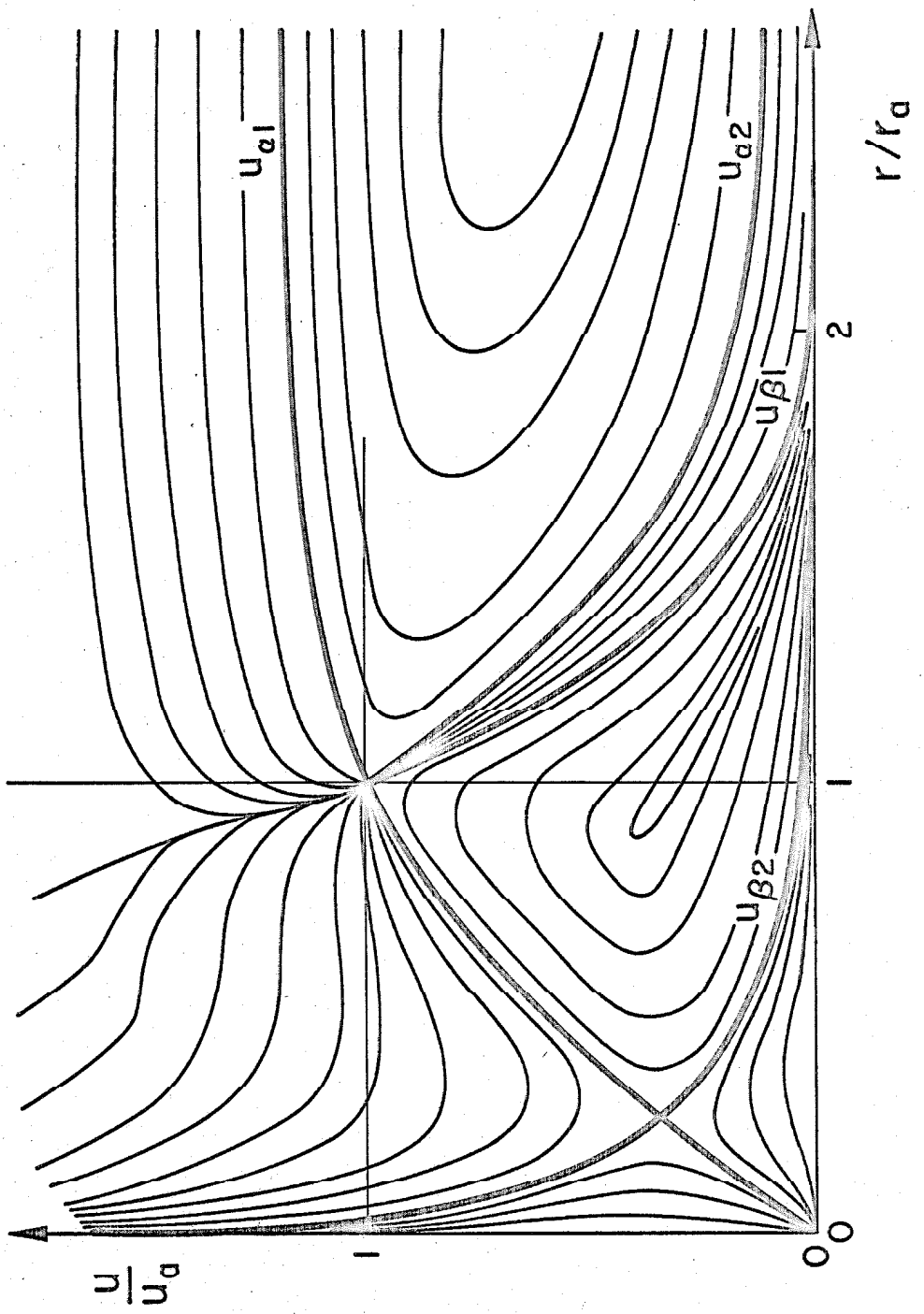

FIGURE III.3.1

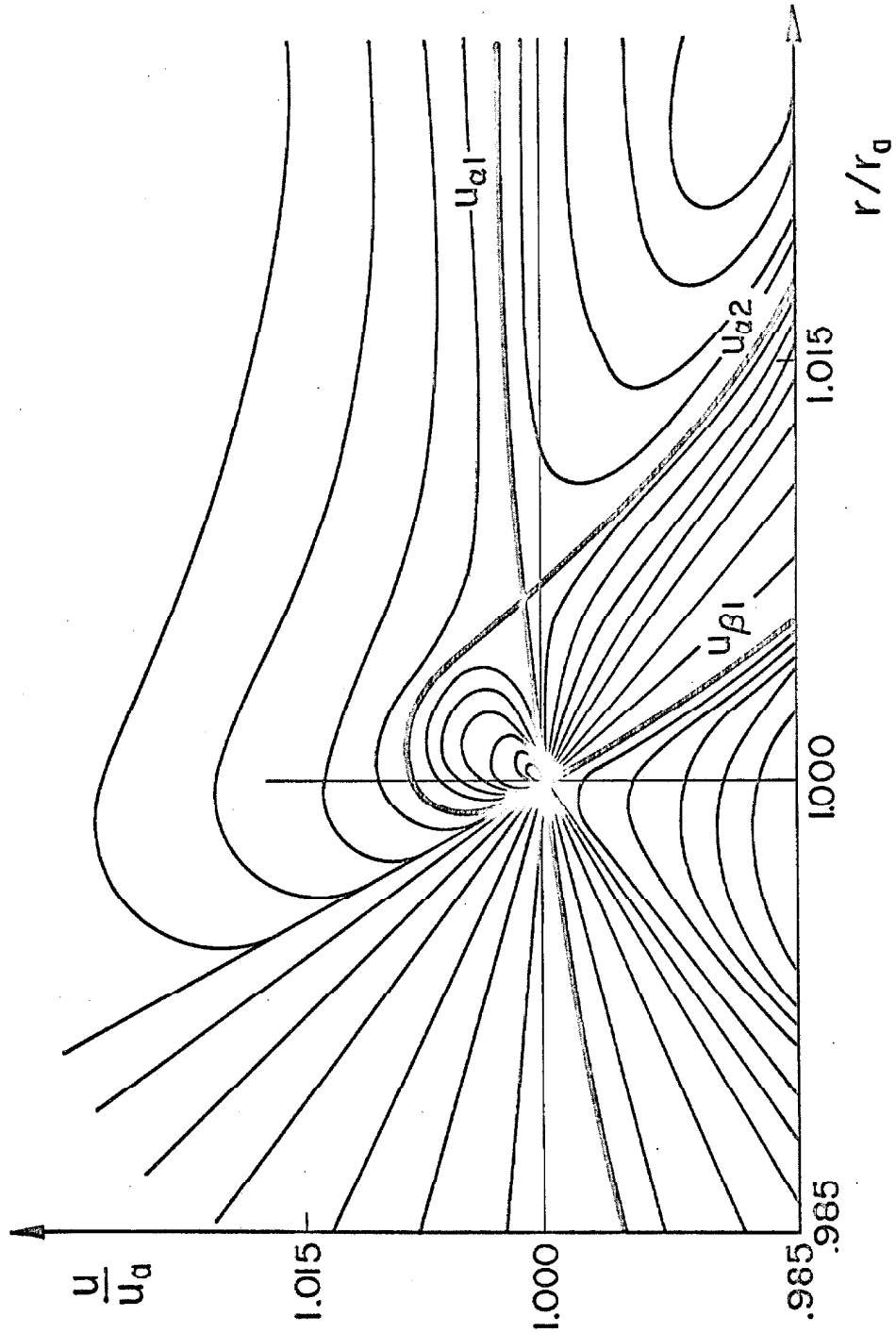

FIGURE III.3.2

at points where the flow velocity equals the velocity of a characteristic wave disturbance in the fluid. For a model without magnetic effects as discussed by Parker (1963) there will be only one critical point which will be close to r_c. There the fluid velocity will equal the sound velocity. If magnetic fields are present, there exist other possible wave fronts besides those formed by sound waves. In magnetohydrodynamics, disturbances may travel in addition as Alfvén waves and the structure of the characteristic manifold is therefore much more complicated. The direction of the magnetic field establishes a preferred axis and thus introduces anisotropy into the fluid. Friedrichs and Kranzer (1958) have shown that all possible speeds of the longitudinal wavefronts can be determined from the characteristic condition. The characteristic condition is

$$w^2[w^4 - (v_{AT}^2 + v_s^2)w^2 + v_s^2 v_{AN}^2] = 0 \qquad \text{(III.3.10)}$$

where w is the velocity of the disturbance relative to the fluid; $v_s = (2\gamma kT/m)^{1/2}$ is the local sound velocity; $v_{AT} = [(B_r^2 + B_\varphi^2)/4\pi\rho]^{1/2}$ is the local Alfvén velocity; and $v_{AN} = (B_r^2/4\pi\rho)^{1/2}$ is the local Alfvén velocity along the component of the magnetic field normal to the wavefront of interest, i.e., the radial Alfvén velocity in our model. All these quantities vary with r. In the region between the surface of the sun and the critical radius r_a, the angle $\delta(r)$ between the magnetic field vector and the radius vector ranges from a very small value to approximately 1/7 radian. Thus $B_\varphi \simeq -\delta B_r$ and to lowest order in δ we can solve Eq. (III.3.10) for the characteristic disturbances

$$w = 0,\ \pm v_s \left(1 - \frac{v_{AN}^2}{2(v_{AN}^2 - v_s^2)}\,\delta^2\right)\ ;\ \pm v_{AN}\left(1 + \frac{v_{AN}^2}{2(v_{AN}^2 - v_s^2)}\,\delta^2\right) \qquad \text{(III.3.11)}$$

This is valid as long as v_{AN} is not close to v_s, which is the case for the sun. We can see from (III.3.11) that there are thus two separate wavefronts traveling with two different possible velocities, a "slow" wave and a "fast" wave.

The set of equations describing the motion of the disturbance is in this case a first order system of hyperbolic equations, from which the characteristics can be obtained as

$$\frac{dr}{dt} = u \pm w \qquad \text{(III.3.12)}$$

It is along these characteristics that all small scale disturbances travel in the solar wind, except those which travel with the solar wind, i.e., which have $w = 0$. Figure III.3.3 shows a sketch of the characteristics in the r-t plane.

At r_c, the fluid velocity is equal to the velocity of the "slow" wave, or the sonic wave and at r_f, u is equal to the velocity of the "fast" wave. These then are the two critical points besides r_a, which we have in the solution of this model.

III.4 Numerical Solution of the Equations

By integrating all the differential equations of motion, we have considerably simplified the problem, but it is still necessary to use machine computations to obtain a specific solution of the algebraic equations that remain. It is necessary to determine values for the

Figure III.3.3

A sketch showing the characteristics in the r-t plane. The characteristics for the "fast" wave are shown in heavy lines, and for the "slow" wave in light lines. The solid lines refer to the solution of Eq. (III.3.12) with the + sign and the dashed lines refer to the - sign. r_o refers to the base of the corona.

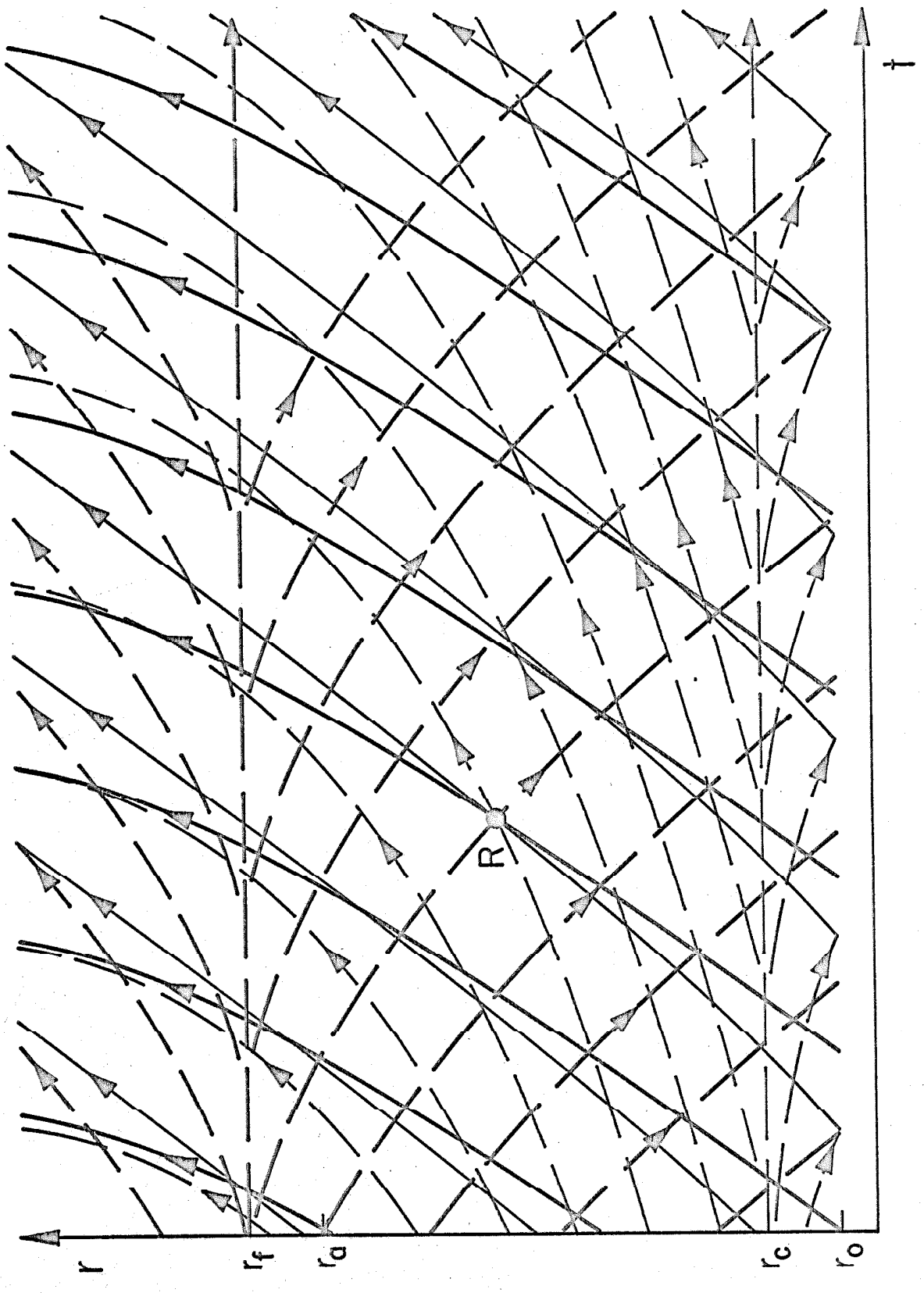

FIGURE III.3.3

various parameters such as the total mass and energy fluxes, and the critical radius and velocity, r_a and u_a. In addition, boundary conditions are needed at r_o to determine the radial magnetic field, pressure and density at this point. Finally, we have to choose a value of γ which will then determine where and how much energy is supplied to the expanding solar atmosphere. A major difficulty is the determination of values for all these quantities that are mutually consistent, that lead to a physically possible solution passing through all three critical points and that correspond to typical solar conditions. The boundary conditions could in principle be determined near the surface of the sun, but we prefer to set r_o = 1 a.u. and determine them at the orbit of earth on the basis of observations from recent interplanetary probes. The subscript $(\ )_e$ rather than $(\ )_o$ is used for these parameters. We assign values for our model that are reasonably typical of conditions in 1964; somewhat different values could have been used without causing important changes. These values were

$$\begin{aligned} u_e &= 400 \text{ km sec}^{-1} \\ B_{re} &= 5\ \gamma \\ \rho_e &= 11.7 \times 10^{-24} \text{ grams cm}^{-3}, \text{ i.e., } 7 \text{ protons cm}^{-3} \\ T_e &= 2 \times 10^5\ ^oK \\ \Omega &= 3.0 \times 10^{-6} \text{ radians sec}^{-1}. \end{aligned} \qquad \text{(III.4.1)}$$

Having thus specified the total mass flux, we cannot independently specify γ, since to obtain the mass flux, a specific energy supply is required and this implies a specific, as yet unknown value of γ.

This can also be seen from a purely mathematical point of view.

We have specified $p_e/\rho_e = 4.7 \times 10^{18}$ erg gm^{-1} and the constant $\rho u r^2 = 1.05 \times 10^{11}$ gm sec^{-1} ster^{-1}; $GM_\odot$ is 1.33×10^{26} dynes cm^2 gm^{-1}. By using Eqs. (II.2.18), (III.2.1) and (III.2.4) we get

$$\frac{2kT_a}{m} = \frac{p_a}{\rho_a} = \frac{p_e}{\rho_e}\left(\frac{\rho_a}{\rho_e}\right)^{\gamma-1} = \frac{2kT_e}{m} M_{Ae}^{2(\gamma-1)} = \frac{2kT_e}{m}\left(\frac{4\pi\rho_e u_e^2}{B_{re}^2}\right)^{\gamma-1} \qquad \text{(III.4.2)}$$

In order to be able to use Eq. (III.2.15) to obtain a solution we must first find r_a, u_a, F and γ. However, unless our solution passes through all three critical points it cannot extend from very small to very large values of r. Thus there must be three pairs of values of (r,u) each of which makes both the numerator and denominator of Eq. (III.2.12) become equal to zero. The pair (r_a, u_a) of course does this, but we must find two more pairs, (r_c, u_c) and (r_f, u_f) that also do this. This gives us 4 equations, but we now have 8 unknowns. In addition, the energy equation must be satisfied at $r = r_a$, r_c, r_f, and r_e and we have thus the necessary 8 equations. If we had tried to specify γ, i.e., the power supply, the system of 8 equations would be over-determined unless we regarded u or ρ at $r_o = r_e$ as unknown. Since the 8 equations are non-linear, there might be more than one solution. We have proceeded by an iterative procedure of machine calculations to find one set which appears to be satisfactory and have assured ourselves that there is no other physically acceptable solution for the given set of boundary conditions.

The equations of motion of the solar wind are greatly simplified and better adapted for machine calculations if they are rewritten in dimensionless form. Let us define new variables as follows:

$$x = r/r_a \tag{III.4.3}$$

$$y = u/u_a \tag{III.4.4}$$

$$z = M_A^2 = x^2 y \tag{III.4.5}$$

Since all constants are evaluated at the earth's orbit, it is convenient to define the radial Alfvénic critical radius as a fraction of 1 a.u., i.e.,

$$\alpha = r_a/r_e = x_a/x_e \tag{III.4.6}$$

Since z is equal to unity at $r = r_a$, the velocity at the Alfvénic critical point is immediately given by

$$u_a = u_e \left(\frac{x_e}{x_a}\right)^2 \frac{1}{z_e} = \frac{u_e}{z_e} \frac{1}{\alpha^2} \tag{III.4.7}$$

It is also convenient to introduce the constants

$$S_\Omega = \frac{\Omega^2 r_a^2}{u_a^2} \tag{III.4.8}$$

$$S_T = \gamma(p_a/\rho_a^\gamma) \frac{1}{u_a^2} \tag{III.4.9}$$

$$S_G = \frac{GM_\odot}{r_a u_a^2} \tag{III.4.10}$$

Using the above equations, the radial momentum equation (III.2.12) takes the dimensionless form

$$\frac{dy}{dx} = \frac{N(x,y)}{D(x,y)} \tag{III.4.11}$$

where the numerator function is given by

$$N(x,y) = (2S_T z^{1-\gamma} - S_G/x)(z - 1)^3 + S_\Omega(y - 1)x^2(x^2y^2 + y - 3z + 1) \tag{III.4.12}$$

and the denominator is

$$D(x,y) = x[(y - S_T z^{-\gamma} x^2)(z - 1)^3 - S_\Omega(1 - x^2)^2 z] \tag{III.4.13}$$

The energy flux equation (III.2.15) becomes

$$F = u_a^2 \rho u r^2 \left\{ \frac{1}{2} y^2 + \frac{1}{\gamma - 1} S_T z^{1-\gamma} - S_G/x + S_\Omega \frac{[(z-1)^2 + (2z-1)(1-x^2)^2]}{2x^2(z-1)^2} \right\} \tag{III.4.14}$$

In a similar way, the expressions for the azimuthal velocity and magnetic field can be brought into the simpler forms

$$B_\varphi(x,y) = - B_{ra} \frac{\Omega r_a}{u_a} \frac{1}{x} \frac{(1 - x^2)}{(1 - z)} \tag{III.4.15}$$

$$v_\varphi(x,y) = \Omega r_a \, x \, \frac{(y - 1)}{(z - 1)} \tag{III.4.16}$$

The essential dimensionless parameters on which the character of the solution depends are γ, $f = F/(u_a^2 u \rho r^2)$, S_T, S_G, and S_Ω. If these are the same for two models, one will find that u/u_a, i.e., y, is the same function of r/r_a, i.e., x, in both. Thus, if these essential parameters are held constant, ρ_a, u_a and r_a may be varied independently to generate a 3 parameter family of equivalent solutions. It is difficult to replace r_a and γ by more directly observable quantities and thus there is no easy way to predict whether two different sets of observed boundary conditions at $r_o \gg r_a$ correspond to essentially the same solution without working out one solution in detail.

In determining a numerical solution, we will find that this model is plagued by the same difficulties which have been experienced by other simpler models which use the polytropic approximation to the energy equation, namely that it is impossible to reproduce the physical conditions both at the earth and at the sun. This model uses the boundary conditions at the earth, with the consequence that at the sun, the radial wind velocity is still very high, the temperature is 2.7×10^6 °K and the density is only 3×10^7 particles cm^{-3}. Values resembling more closely those known to exist at the sun can be obtained by using a slowly varying polytropic index γ between the sun and the critical point. But this is just another way of saying that the energy supply given by any constant γ is incorrect. We can improve the model by using a slowly varying γ, where γ approaches a value close to 1 near the sun's surface. This will yield a much better fit for the conditions in the coronal region.

The solution corresponding to the boundary conditions (III.4.1) yields $\gamma = 1.221$, $r_a = 24.3\ r_\odot$, i.e., $\alpha = 0.1131$, $u_a = 3.32 \times 10^7$ cm sec^{-1}, $r_c = 3.0\ r_\odot$, $u_c = 1.82 \times 10^7$ cm sec^{-1}, $r_f = 24.6\ r_\odot$, $u_f = 3.33 \times 10^7$ cm sec^{-1}, and $F/\rho u r^2 = 9.02 \times 10^{14}$ ergs gm^{-1} sec. The determination of u as a function of r, and from this all other properties of the solution, follows by direct numerical solution of the algebraic equation (III.4.14). The radial velocity is shown in Figure III.4.1. For comparison, this figure also shows the radial Alfvénic velocity v_{AN} and the sound velocity. The density profile is shown in Figure III.4.2. The temperature of the gas predicted by this model is indicated in Figure III.4.3. As soon as the

Figure III.4.1

The solution of the radial velocity u from the polytrope model. For comparison the radial Alfvénic velocity v_{AN} and the local sound velocity v_s are also shown. The critical point r_c is very close to the intersection of the curves u and v_s, whereas the other two critical points r_a and r_f are at and very near the point where $u = v_{AN}$.

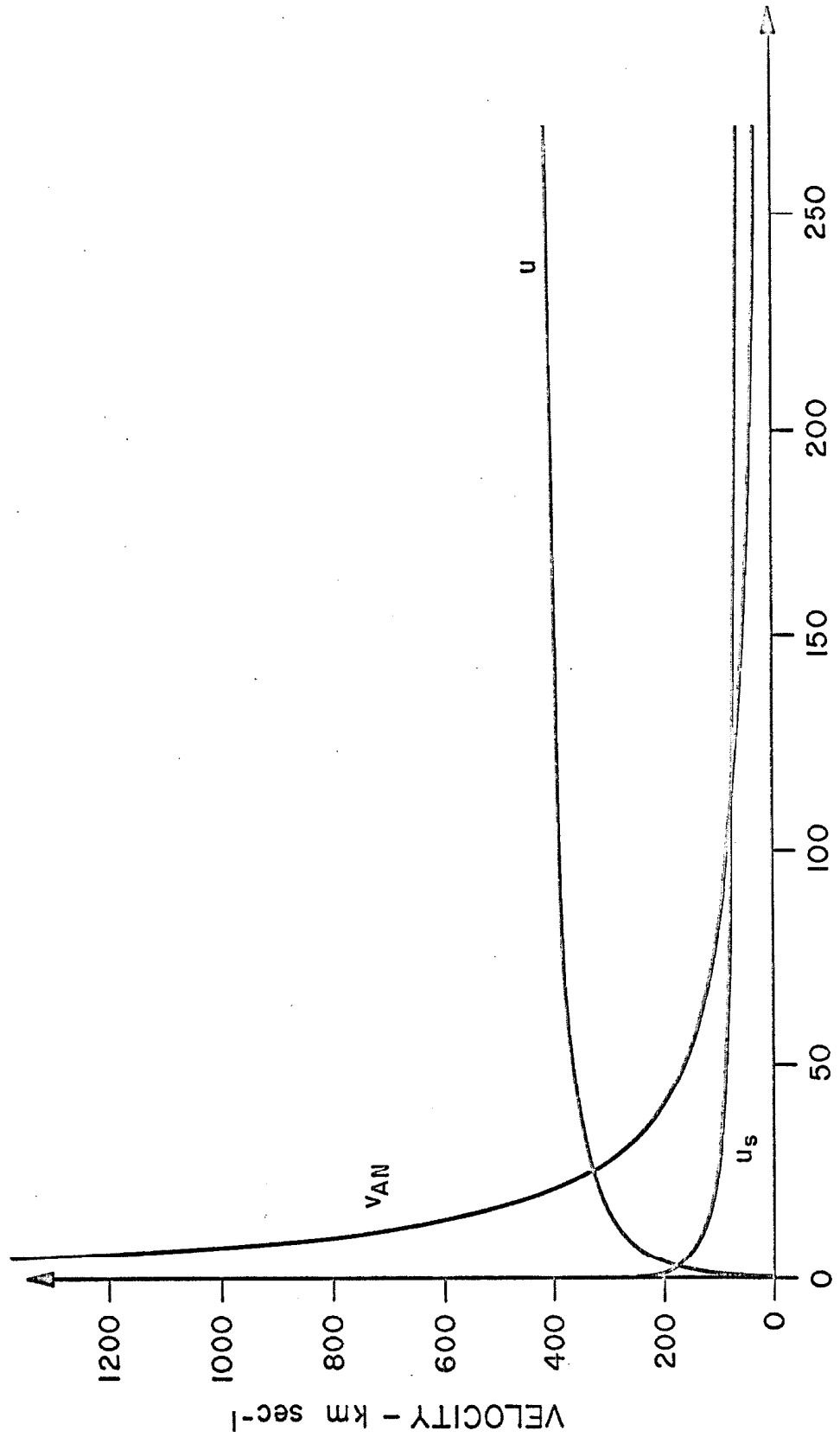

FIGURE III.4.1

Figure III.4.2

Solar wind density profile derived from the polytrope model

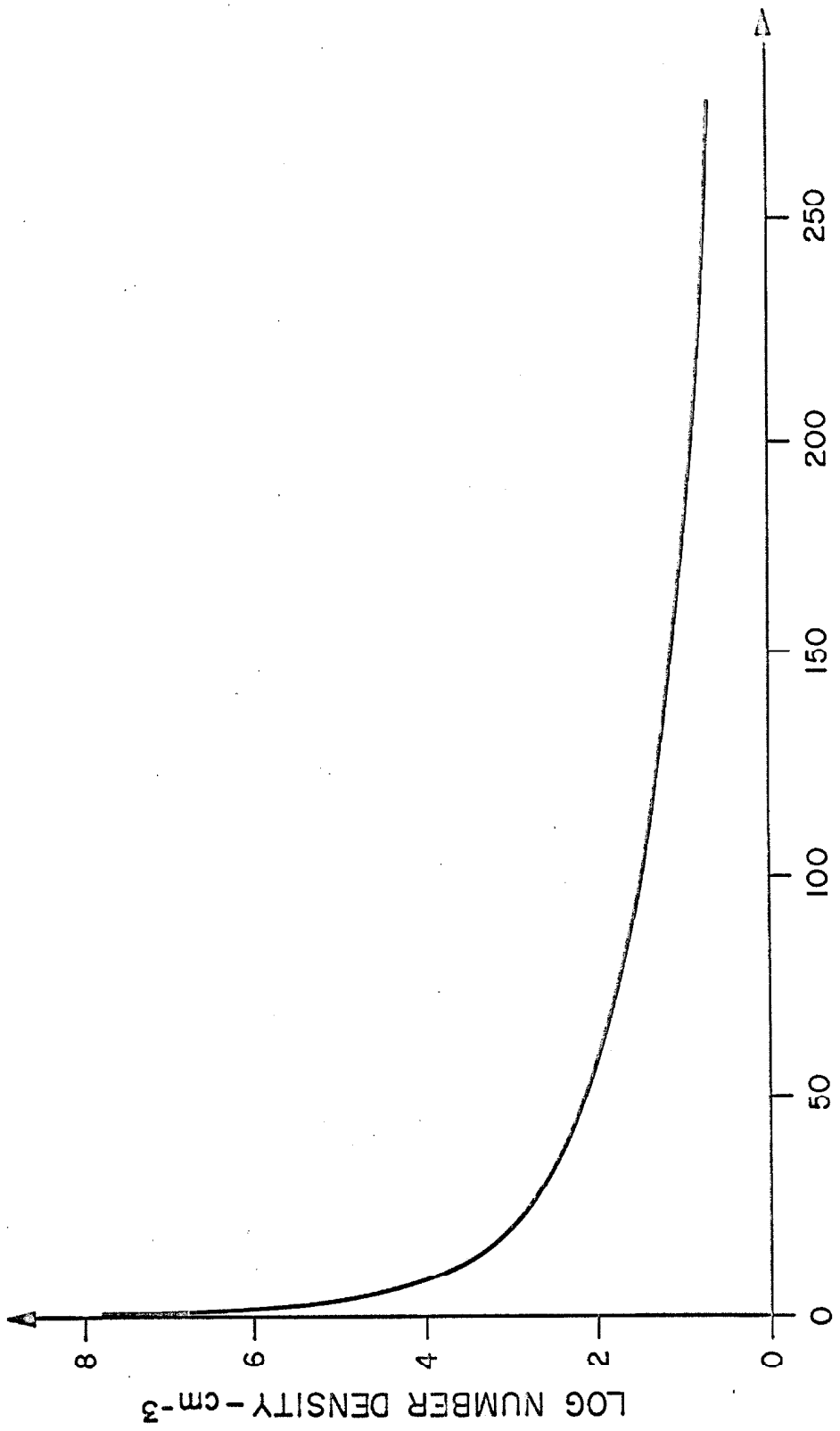

FIGURE III.4.2

Figure III.4.3

Solar wind particle temperature profile from the polytrope model.

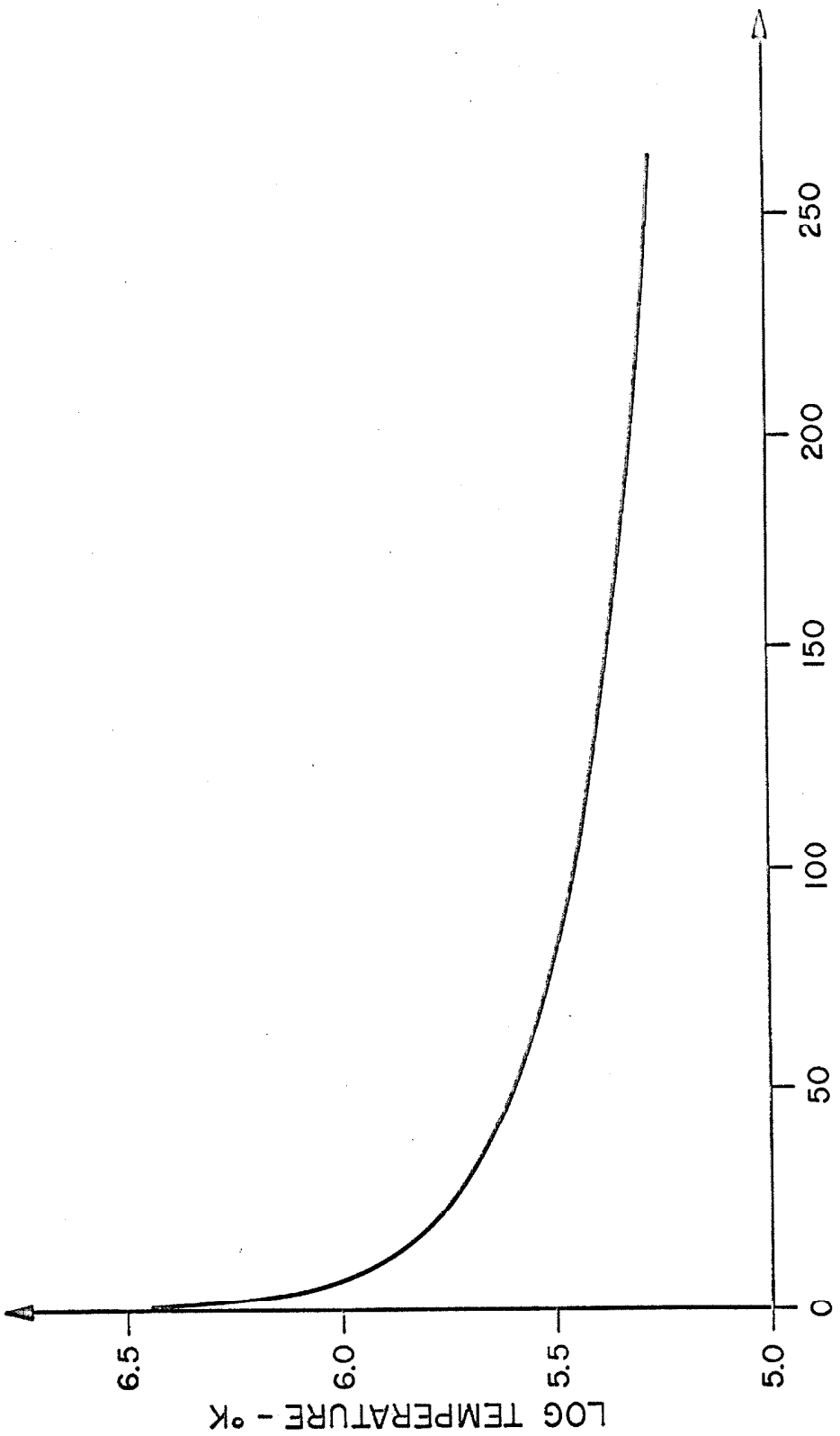

FIGURE III.4.3

radial velocity and the Alfvénic critical points are known, the azimuthal magnetic field can be calculated and the result is indicated in Figure III.4.4. On the same graph we have also shown for comparison the radial magnetic field component. The result shows clearly the $1/r$ dependence of B_φ as compared to the $1/r^2$ dependence of B_r.

In this connection it is of considerable interest to determine the pattern which the magnetic field produces in interplanetary space. If (r,ψ) are the polar coordinates of points along the magnetic field lines, then $\psi(r)$ must satisfy the equation

$$\frac{r d\psi}{dr} = \frac{B_\varphi}{B_r} \qquad \text{(III.4.17)}$$

which we can integrate to obtain

$$\psi(r) - \psi_o = \int_{r_o}^{r} \frac{B_\varphi dr}{rB_r} = \frac{\Omega r_a}{u_a} \int_{x_o}^{x} \frac{1 - x^2}{1 - z} dx \qquad \text{(III.4.18)}$$

where ψ_o is a constant of integration. The result is shown in Figure III.4.5. The spiral pattern of the magnetic field in the equatorial plane resembles very closely the Archimedes spiral given by Parker (1963) and shows no anomalies at the Alfvénic critical point. For example, a line of force spirals 62^o in solar longitude between the surface of the sun and 1 a.u. The magnetic field vector is almost radial near the solar surface and makes an increasingly larger angle with the radius vector as the distance from the sun increases. The change in this angle, commonly called the "hose" angle is shown in Figure III.4.6. From it we can see that the magnetic field near 1 a.u. makes approximately an angle of 45 deg. with the radial direction.

Figure III.4.4

The magnetic field components in interplanetary space. B_r is the radial component and B_φ the azimuthal component of the magnetic field vector. The curve labeled N is the B_φ component for the non-viscous, isotropic model whereas the curve labeled V refers to the solution of B_φ for the viscous, anisotropic model treated in Section IV.

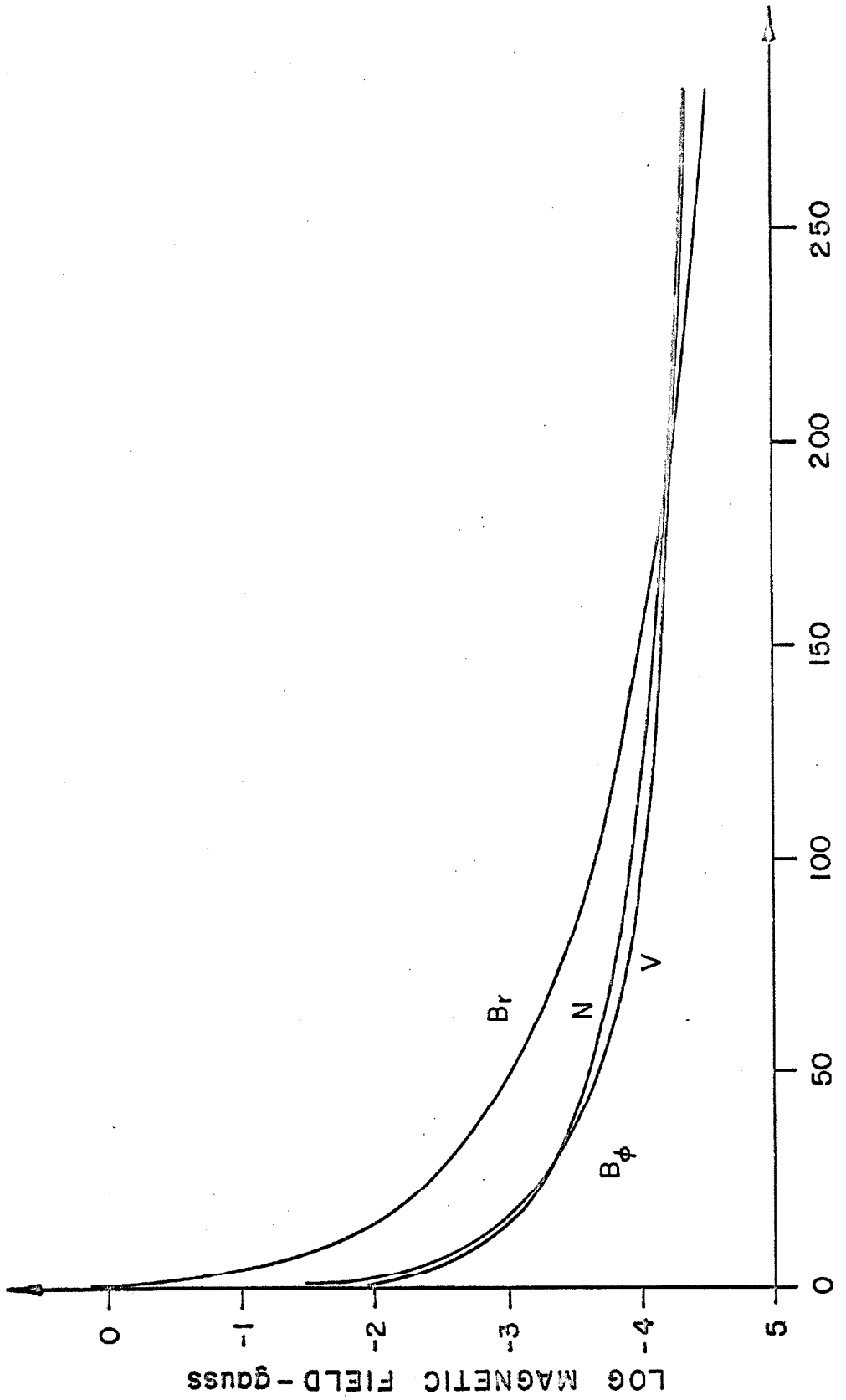

FIGURE III.4.4

Figure III.4.5

Equatorial magnetic field pattern swept out by the solar wind. The spiral resembles the one obtained by Parker (1963), for which he assumed rigid corotation of the plasma to a certain radius and no azimuthal wind velocity from then on, but differs from it since the actual radial dependence of B_φ was used.

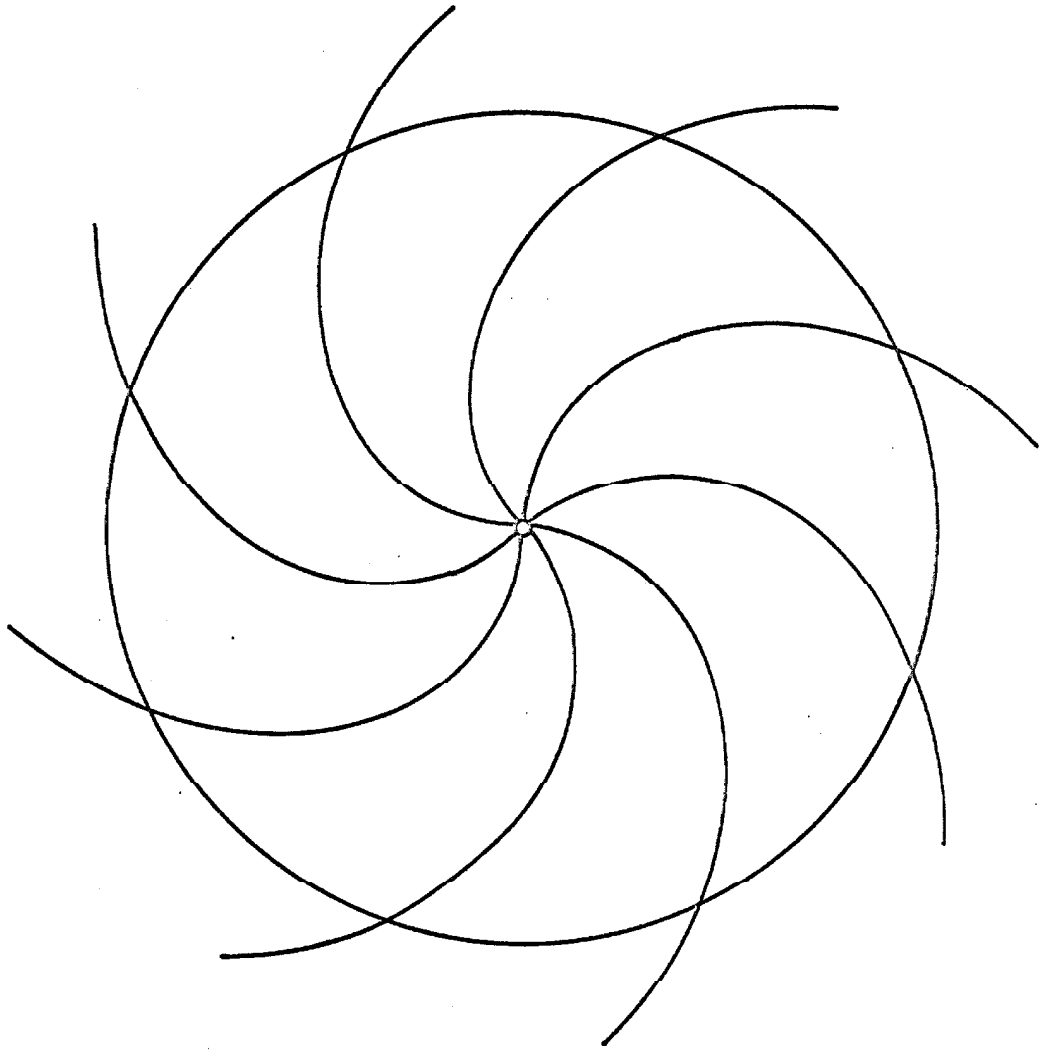

FIGURE III.4.5

Figure III.4.6

The magnitude of the "hose angle", the angle which the magnetic field vector makes with the radius vector. In the neighborhood of the sun this angle is strongly dependent on the azimuthal velocity of the wind, whereas near 1 a.u. the magnitude of the hose angle is given by $\tan^{-1}(\Omega r/u)$ with a maximum error of approximately 1%.

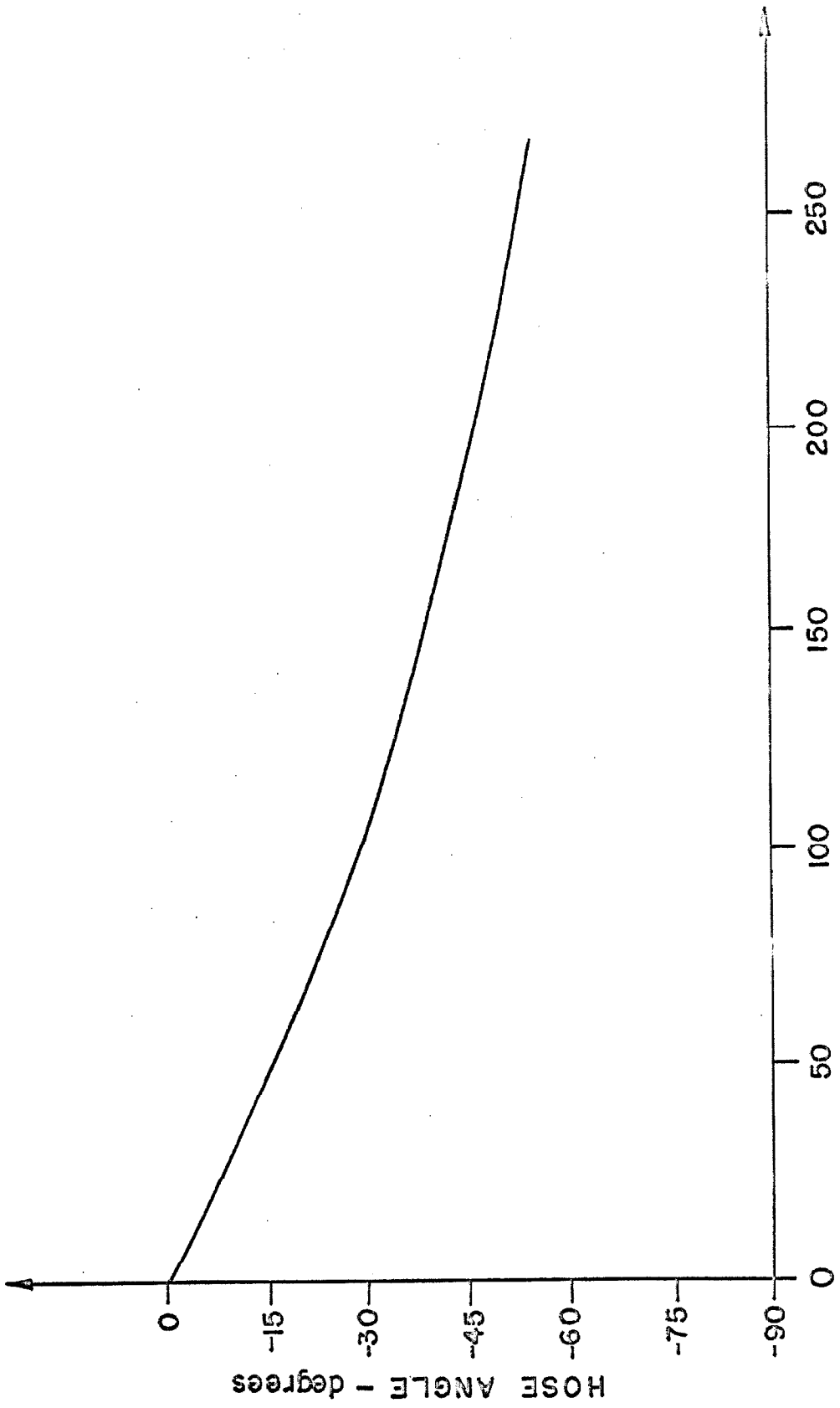

FIGURE III, 4.6

Certain time varying features of the magnetic field which have their origin in the vicinity of magnetically active regions on the surface of the sun are associated with the lines of force originating in this region and can be observed by space probes. Such active regions are also the origin of high and low velocity plasma jets which have been observed. It is thus of interest to know the elapsed time $(\psi(r) - \psi_o)/\Omega$ between the passage of the foot of a line of force on the sun beneath the subsolar point of an observer at a distance r from the sun, and the passage of the actual line of force past the observer. This is indicated by curve 1 in Figure III 4.7. Curve 2 on the same figure shows the transit time t(r) which the plasma requires to reach any given point in space. We obtain the transit time from

$$t(r) - t_o = \int_{r_o}^{r} \frac{dr}{u} \qquad \text{(III.4.19)}$$

where t_o is again a constant of integration. This transit time is again important in that it allows us to make a prediction when disturbances traveling with the bulk velocity of the plasma reach any given point in space. At 1 a.u. the elapsed time $(\psi(r_e) - \psi_o)/\Omega$ is only 4.65 days, compared to the plasma transit time of 5.65 days.

The transit time is quite sensitive to the details of the model just above the sun's surface, since the plasma has a low velocity in this region and thus spends a relatively long time there. In contrast, the elapsed time shown in curve 1 is almost completely insensitive to the exact behavior of the radial velocity in this region.

The dependence of the azimuthal velocity on radius is shown in

Figure III.4.7

The solid curve gives the total time required between the central meridian passage of the photospheric foot of a line of force, assuming the model is valid clear to the photosphere, and the passage of this line of force past any given point r.

The dashed line indicates the total transit time of the plasma from the time it left the sun's surface until it reaches any given point r.

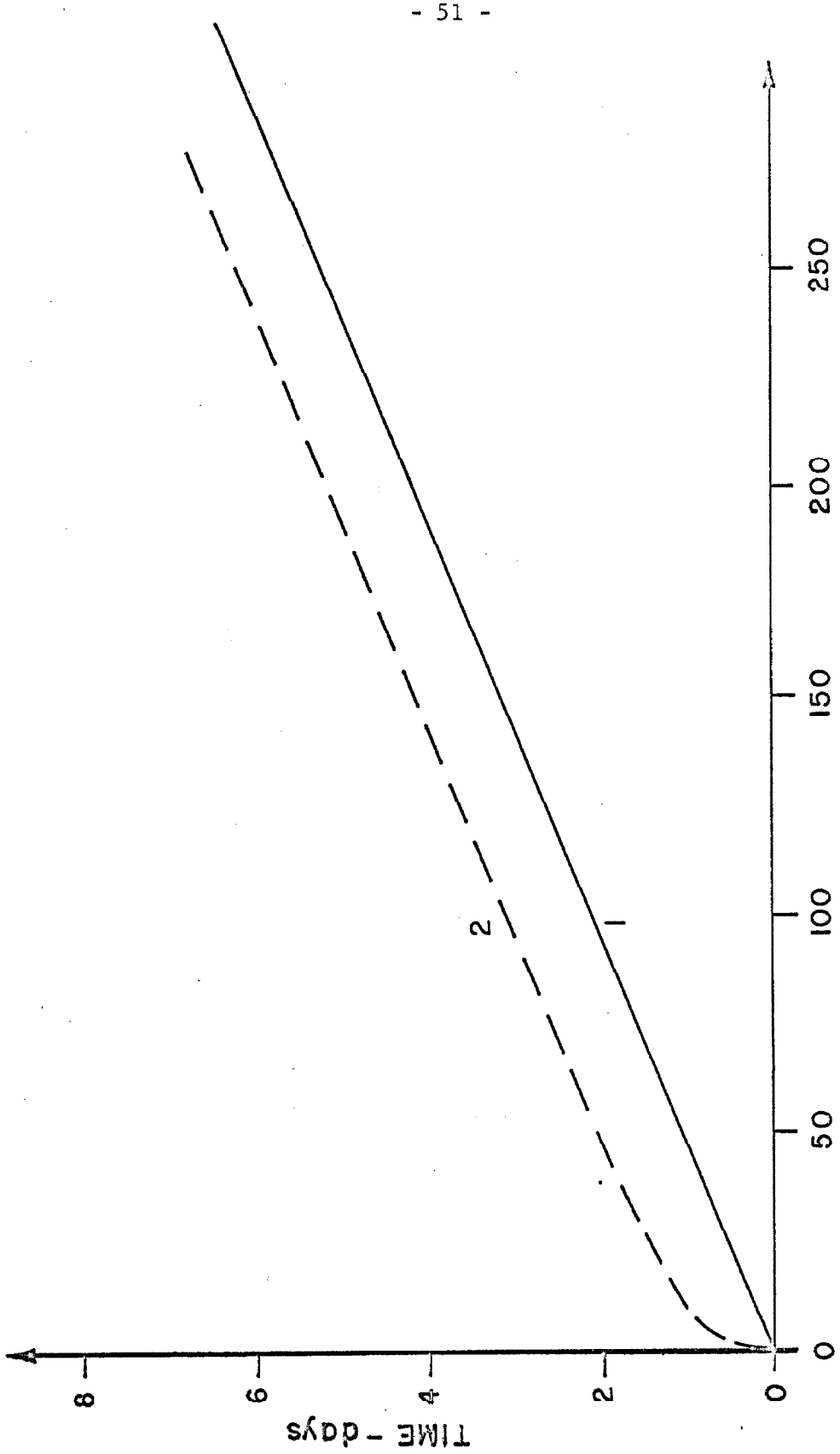

FIGURE III.4.7

Figure III.4.8. It approaches the sun's velocity at $r_\odot$, increases to a maximum value nearly twice as high at approximately $12r_\odot$ and then declines. The increase in azimuthal velocity is never as rapid as though there were strict corotation with the sun, the angular velocity at $12r_\odot$ being only about 0.16 that at the surface. The angular momentum convected by the solar wind increases monotonically with radius as indicated in Figure III.4.9, but never produces nearly as large an effect as the torque due to the magnetic field, which is shown for comparison in the same figure. The sum of the angular momentum loss and the torque on the sun is a constant and represents the total angular momentum loss of the sun per gram of matter lost due to the solar wind, which amounts to 8.67×10^{18} cm^2 sec^{-1}. Together with a total mass flux of 1.054×10^{11} gm sec^{-1} steradian this represents a loss to the angular momentum of the sun of 9.15×10^{29} dynes-cm steradian^{-1}. This will have a decelerating effect on the angular motion of the sun. To obtain this braking torque, we need only to assume that the calculations made for the equatorial region apply to the entire surface, except that the factor sin θ is inserted for the latitude dependence. The total rate of change of $J_\odot$, the total angular momentum of the sun can then be written as

$$\frac{dJ_\odot}{dt} = \frac{2}{3}\Omega r_a^2 \frac{dM_\odot}{dt} = -\frac{J_\odot}{\tau} \qquad \text{(III.4.20)}$$

where τ is a characteristic time, which for this particular model turns out to be about 7×10^9 years for a uniformly rotating sun. Thus the solar wind should have a substantial influence on the total angular momentum of the sun.

Figure III.4.8

Azimuthal velocity of the solar wind. If there were rigid corotation the azimuthal velocity would increase proportional to r, whereas if the angular momentum would be conserved, the azimuthal velocity would decrease inversely proportional to r. In the actual solar wind, the azimuthal velocity increases for some distance and then declines. The increase is much less than one would obtain for the case of a corotating gas. For this model the maximum azimuthal velocity is at 11.5 $r_{\odot}$, where its angular velocity is only 16% of the solar angular velocity. Near 1 a.u. the azimuthal velocity falls off very nearly inversely proportional to r.

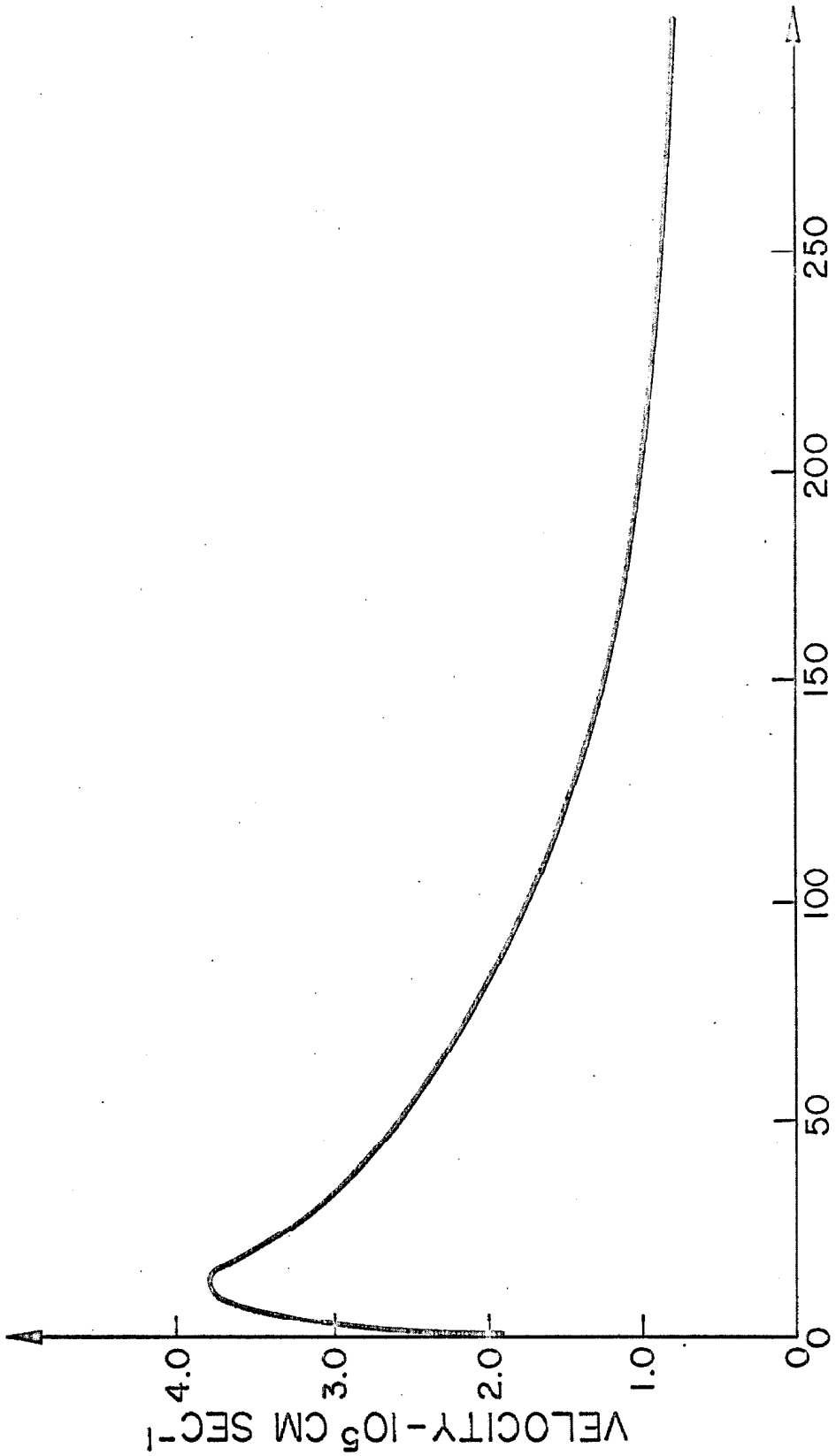

FIGURE III.4.8

Figure III.4.9

The magnetic torque and the angular momentum in the solar wind. The angular momentum convected by the solar wind increases monotonically with radius but never produces nearly as large an effect as the torque due to the magnetic field. Any increase in the plasma angular momentum is exactly balanced by a decrease in the torque, even though this is not quite apparent from the figure, which shows these quantities on a logarithmic scale. The asymptotic value for rv_φ will be $r_a^2\Omega \cdot (1 - u_a/u_\infty)$ and for the magnetic torque $r_a^2\Omega \cdot u_a/u_\infty$.

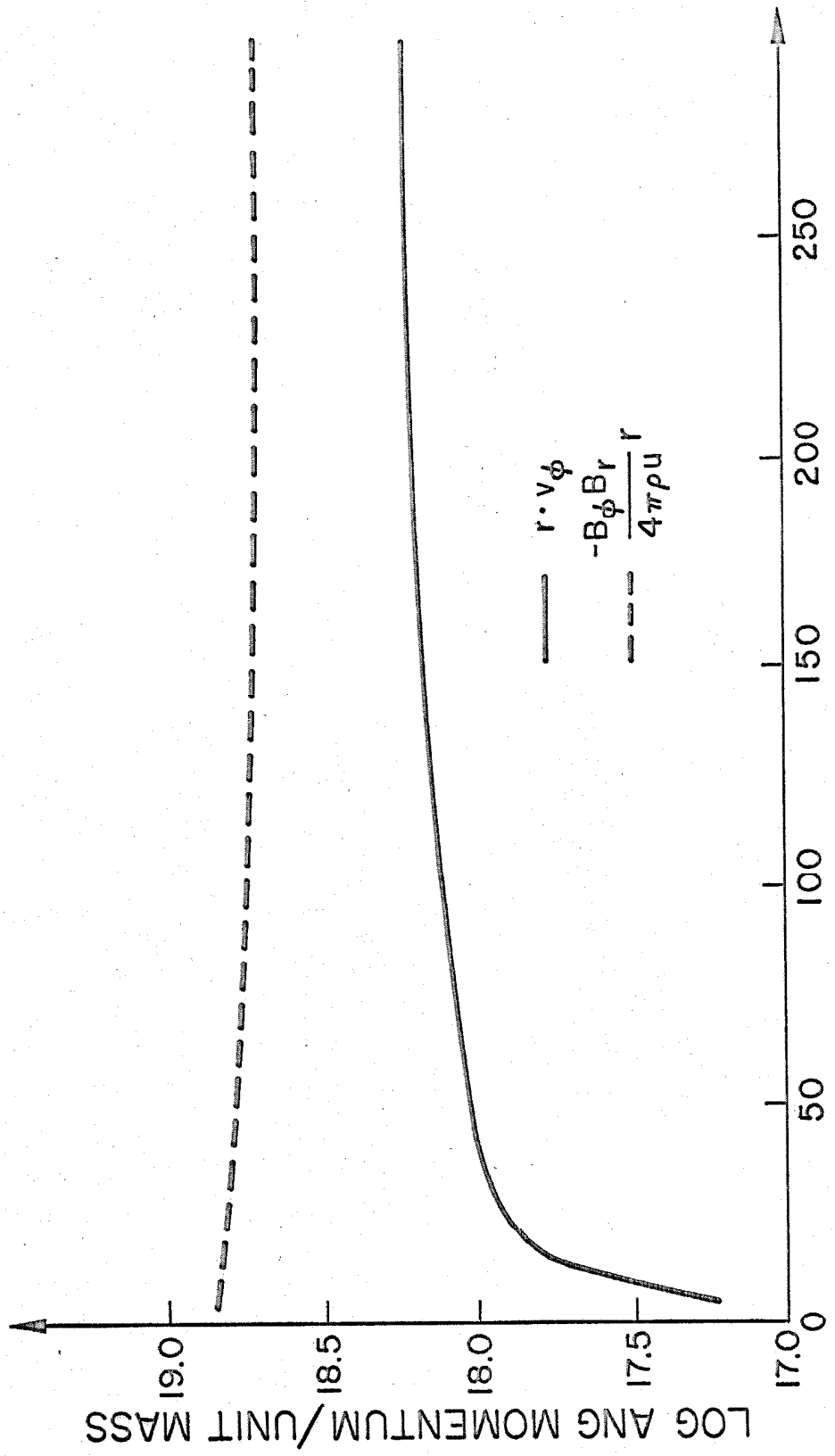

FIGURE III.4.9

The use of a polytropc model implies a specific form for S(r) which is given by

$$S(r) = \rho u \left[\frac{\gamma}{\gamma - 1} M_A^{-2(\gamma-1)} - 5/2\, M_A^{-4/3} \right] \frac{p_a}{\rho_a} + \kappa \frac{dT}{dr} \qquad \text{(III.4.21)}$$

From the solution we have calculated S(r) and the result is indicated in Figure III.4.10.

Polytrope models in which the magnetic and centrifugal force terms have been neglected had been treated earlier by Parker (1958, 1963), Dahlberg (1963) and other investigators and we are now in a position to compare the size of these neglected terms to the pressure, gravitational or inertial terms for the radial motion. If this is done we find that the size of the neglected terms are only of the order of 1% of the size of the other terms. Thus their neglect will not change the general behavior of the radial wind velocity to any significant extent. On the other hand if we wish to apply the theory of the solar wind to the expanding coronas of other stars, especially to highly magnetic stars or to stars with a large surface rotation rate, the model presented here has to be used rather than Parker's model. Although polytrope models have a number of features which definitely do not represent the physical situation accurately, they are models which can be solved or at least understood qualitatively quite readily. In the next section we will discuss a more complicated model, which will allow us to gain some insight into the energy balance of the solar corona itself.

III.5 The Heating of the Solar Corona and the Solar Wind

In using a polytrope model of the solar corona and of the solar wind, we have, as has been shown by Eq. (III.4.21), in fact specified

Figure III.4.10

The convection of thermal energy and the energy deposition into a polytrope solar wind model. $F_T = \frac{\gamma}{\gamma - 1} M_A^{-2(\gamma-1)} \rho u r^2 \frac{p_a}{\rho_a}$ represents the sum of the enthalpy plus the energy transported by thermal conduction, waves, etc. for the polytrope model. $F_E = \frac{5}{2} M_A^{-4/3} \rho u r^2 \frac{p_a}{\rho_a}$ represents the enthalpy convected out by the solar wind, $F_C = - r^2 \kappa \frac{dT}{dr}$ is the energy flux due to thermal conduction alone and $F_S = r^2 S(r)$ is the energy flux which has to be supplied in order that the polytrope approximation be a correct description of the solar wind.

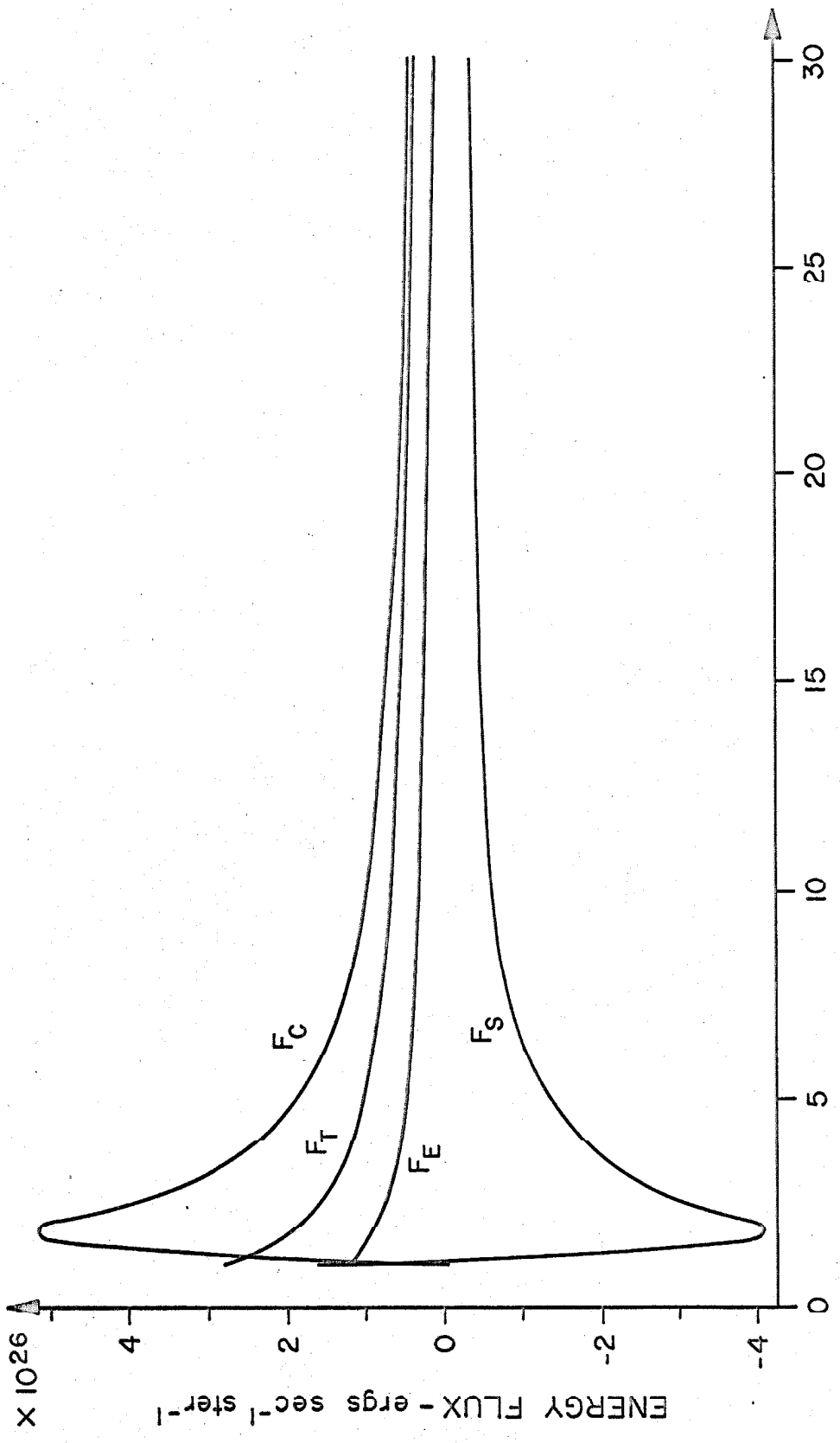

FIGURE III.4.10

how much energy is deposited at any given point. This particular distribution is not readily explained physically and it would be of interest if one could determine a more realistic function S(r) for a study of the solar wind. This would also presumably result in a model of the solar wind more realistic than the polytrope model. If we consider the complete energy equation (II.2.19) for a case in which there is no viscosity and where the pressure is isotropic, σ^{o}_{rr} and p_{rr} are equal to zero. Furthermore we have found in the previous section that the influence of the magnetic field and of the azimuthal motion on the radial motion is very slight. Therefore we neglect the energy carried by the field and in the azimuthal motion compared to the kinetic energy in the radial motion and to the gravitational or thermal energies, i.e., we set v_φ and B_φ equal to zero. With these assumptions the energy flux equation (II.2.19) may be solved for S,

$$S(r) = F/r^2 - \rho u \left\{ \frac{1}{2} u^2 - \frac{GM}{r} + \frac{5kT}{m} \right\} + \kappa \frac{dT}{dr} \qquad \text{(III.5.1)}$$

For this simple model the radial momentum equation is

$$u \frac{du}{dr} = - \frac{GM}{r^2} - \frac{1}{\rho} \left\{ \rho \frac{dT}{dr} + T \frac{d\rho}{dr} \right\} \frac{2k}{m} \qquad \text{(III.5.2)}$$

These two equations could be solved for S(r) if we had some experimental data from which we could determine either the solar wind velocity, density or temperature as a function of radius and a suitable set of boundary conditions. The experimental determination of these solar wind properties, at least in the region between the sun and earth, have not yet been made and, because of their complexity and difficulty, will not likely be made for some time. But solar coronal density data are

available from observations by Van de Hulst (1950), de Jager (1959) and Pottasch (1960) for the region between the chromosphere and 10 $r_\odot$ out. Actual data are shown by these authors for distances to approximately 30 $r_\odot$, but it has been argued by Blackwell and Ingham (1961) that not too much significance should be attached to the values beyond 8 - 10 $r_\odot$.

From physical considerations we expect that in the case of a quiet corona and a quiet solar wind most of the energy carried by waves, and represented by the function S(r), will be deposited in the corona itself, mainly in the region between 1 and 4 $r_\odot$. In particular, we expect that beyond 10 $r_\odot$ the energy carried by waves is negligible compared to the energy carried by the solar wind itself or by thermal conduction. This will not be true in regions where we find plasma jets of different velocities interacting with each other since at their boundaries a large amount of heating may take place. But for quiet solar wind conditions we expect that

$$\left|\kappa \frac{dT}{dr}\right|, \frac{\rho u^3}{2} \gg |S| \qquad \text{(III.5.3)}$$

and thus S(r) may be set equal to zero beyond 10 $r_\odot$. With these assumptions and suitable boundary conditions at 1 a.u. equations (III.5.1) and (III.5.2) can be solved in the region between 10 $r_\odot$ and 1 a.u.

For the region between 1 $r_\odot$ and 10 $r_\odot$ we have used the density distribution as given by Pottasch (1960), which may conveniently be approximated by

$$\rho = \rho_o[(r_o - r_\odot)/(r - r_\odot)]^{7/3} \qquad \text{(III.5.4)}$$

with $\rho_o = 3.8 \times 10^6$ particles cm^{-3} and $(r_o - r_\odot) = 5 \times 10^{10}$ cm.

Figure III.5.1 shows that this equation is a very good approximation to the observed density distribution, except in the lower corona where the true situation is much more complicated and where we would really not gain significant insight into the problem by using a better analytical fit to the experimental data. The solution obtained for the solar wind in the region between 10 $r_\odot$ and 1 a.u. has now to be continued smoothly to the solution in the lower region between 1 $r_\odot$ and 10 $r_\odot$. In this way the function S(r) is determined.

In the actual solution of these equations many problems have to be solved. The coronal density measurements quoted by Pottasch were made over a period of years, mainly between 1953 and 1955. During that time, no solar wind measurements were taken, because the first satellite was only launched in 1957. Thus we have no idea what the typical solar wind values were during the time the coronal observations were taken. If we assume a set of "reasonable " solar wind values, we may find that it is not possible to match the solutions in the two regions, smoothly and continuously. The best solution which we obtained has as boundary values $F = 9.184 \times 10^{25}$ erg sec^{-1} $steradian^{-1}$, $\rho u r^2 = 6.714 \times 10^{34}$ ions sec^{-1}, $u_e = 300$ km sec^{-1}, $\rho_E = 10$ ions cm^{-3}. The resulting temperature at 1 a.u. is 2.4×10^5 ^oK. The general behavior of the solution of the radial solar wind equation does not deviate appreciably from the solution of the polytrope model, except that as r approaches $r_\odot$ the density increases enormously and thus the radial velocity falls off rapidly. This decrease in the radial velocity

Figure III.5.1

The density profile of the solar corona as given by Pottasch (1960). The dashed straight line is the density function $n = n_p[(r - r_p)/(r - r_\odot)]^{7/3}$ which was used in the work of section III.5.

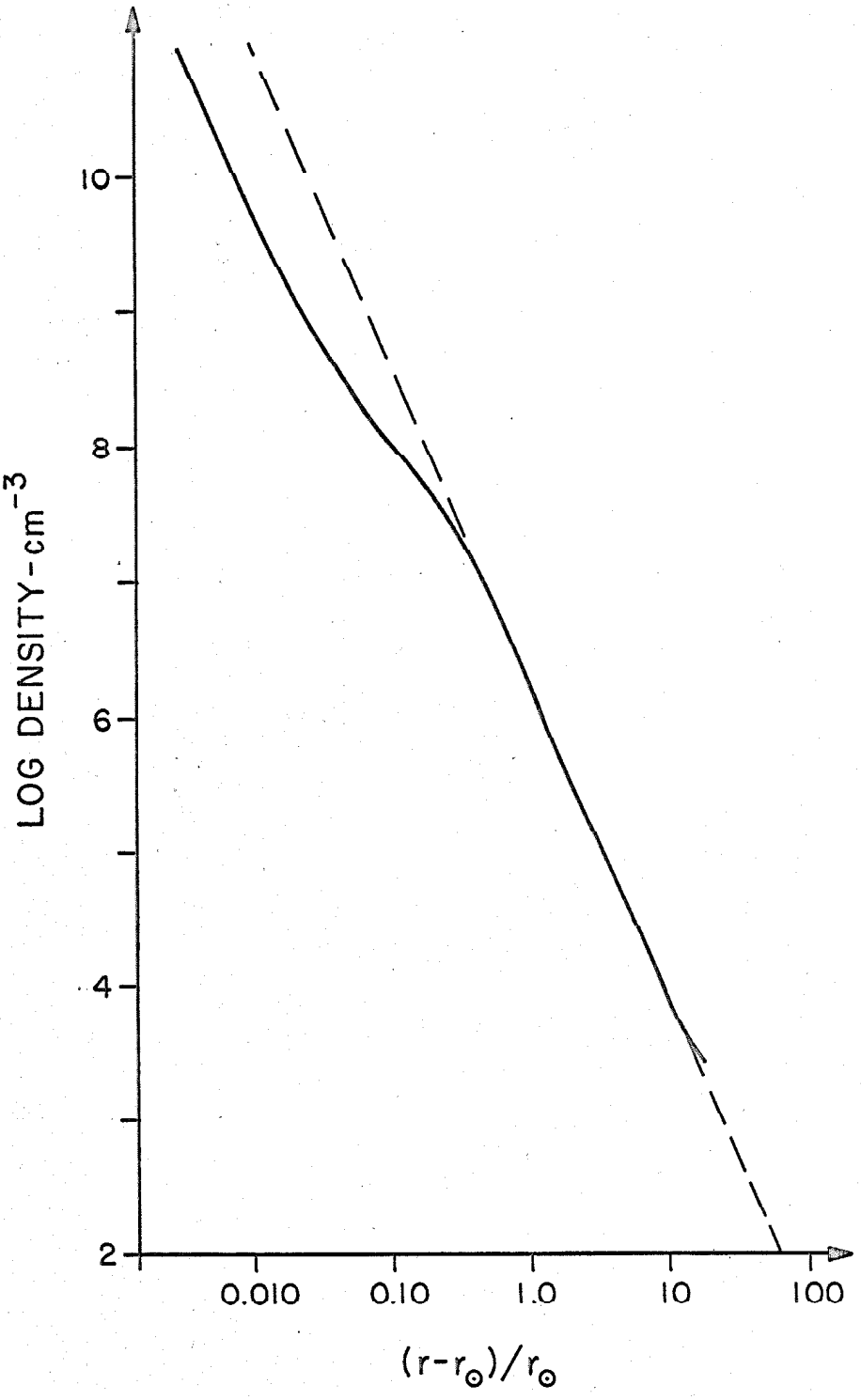

FIGURE III.5.1

is much more pronounced in this model than in the polytropic model, and appears to be more realistic. Another marked difference for this model is the temperature profile in the corona, which is shown in Figure III.5.2. This distribution exhibits the characteristic rise in temperature between the chromosphere and the corona.

Figure III.5.3. shows the various components of the energy flux, with $F_w = \rho u r^2 \left(\frac{1}{2} u^2 - \frac{GM}{r} + \frac{5kT}{m}\right)$ being the energy flux per steradian convected by the solar wind, $F_c = - \kappa r^2 \frac{dT}{dr}$ the energy flux per steradian transported by thermal conduction and $F_s = r^2 S(r)$ the energy flux per steradian due to waves. The dashed lines indicates the total energy flux per steradian, F. From this figure we can see that F_s is only important in the region between the sun and approximately 3.5 $r_\odot$. The exact shape of this function is still uncertain, since the two regions were not matched exactly. Nevertheless, we have shown that the method outlined in this section provides a means of determining the amount and distribution of energy supplied to the solar wind from the dissipation of waves in the corona.

Figure III.5.2

Temperature profile of the solar wind obtained from the solution of the solar wind equation with heat flux for $r \geq 10\ r_{\odot}$ and using the density function given in Figure III.5.1 in the region $r_{\odot} \leq r \leq 10\ r_{\odot}$.

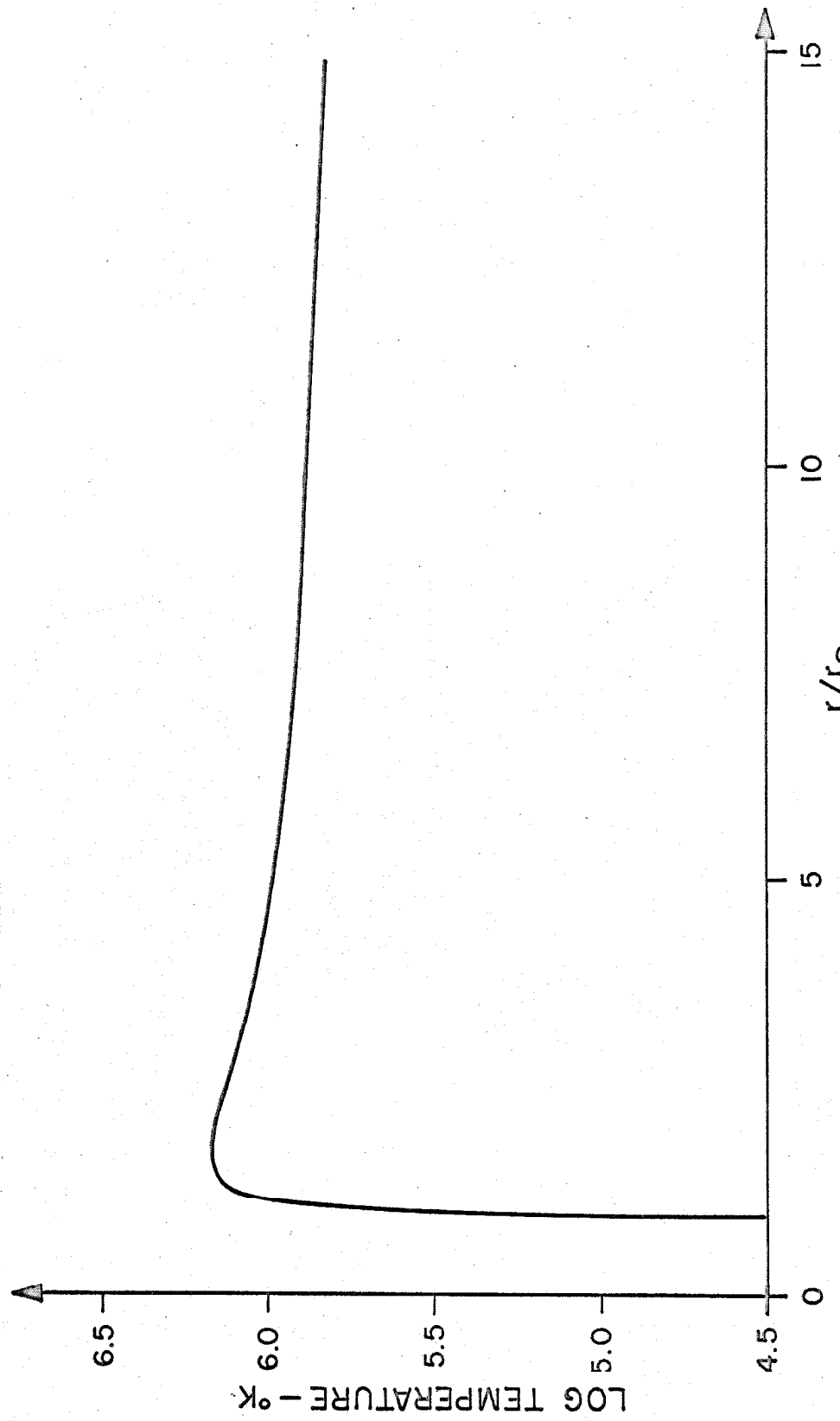

FIGURE III.5.2

Figure III.5.3

The total energy flux F_T and its components. F_W is the energy convected by the solar wind, F_c the energy flux due to thermal conduction and F_s the energy flux in the form of waves.

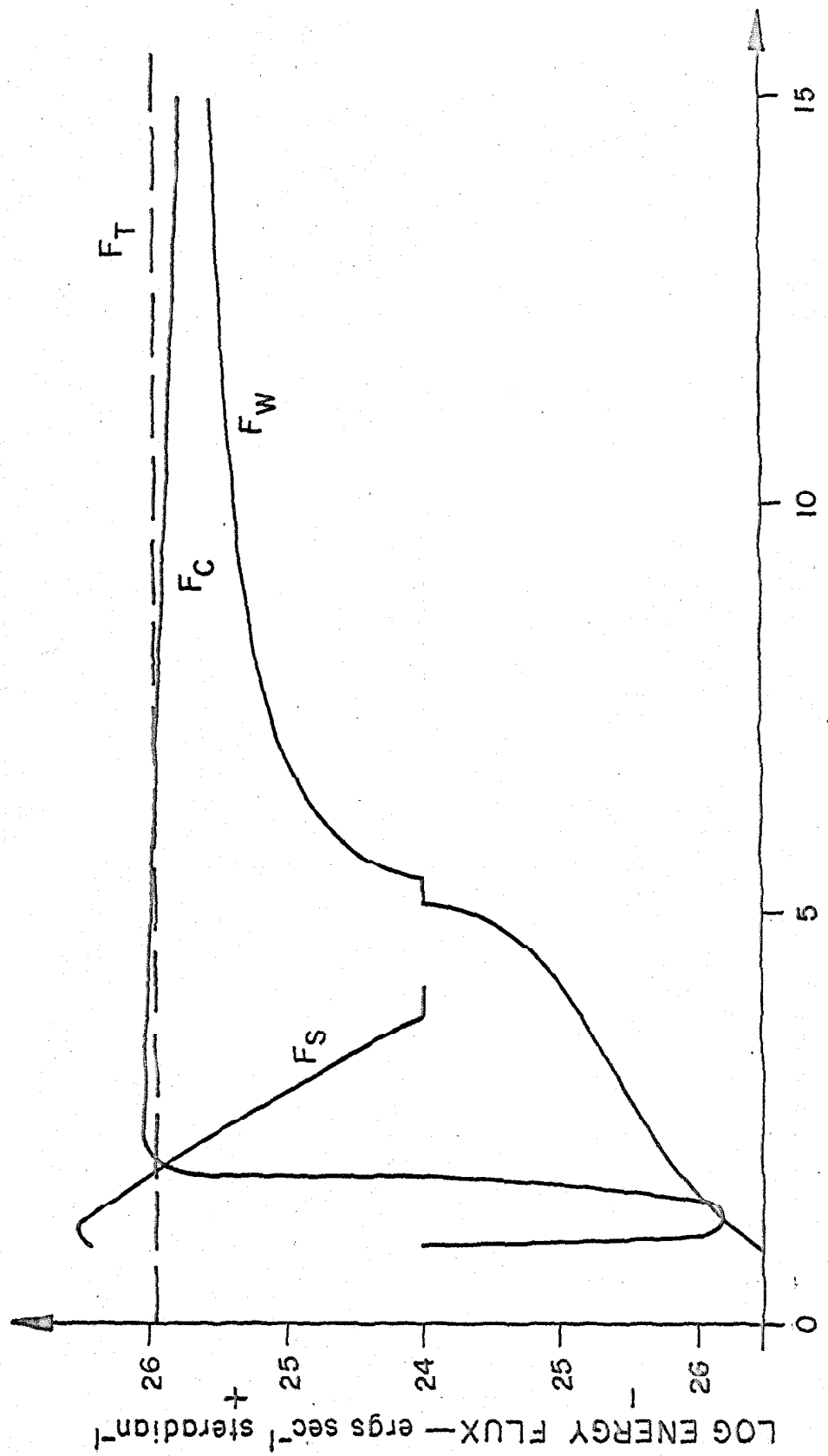

FIGURE III.5.3

3.6 Stability Considerations for the Azimuthal Motion

The complete general problem of the solar wind stability is at the present time too complicated to be solved. Various attempts have been made to discuss specific cases of the stability of the radial motion of the solar wind. Parker (1966) has discussed the stability of his model, in which no magnetic fields are considered. He has shown that no intrinsic instabilities appear as the sole result of the existence of the solar wind. Carovillano and King (1966) have investigated the dynamical stability of the solar wind with boundary perturbations. They considered an expansion of the solar wind in spherical harmonics and they too concluded that the solar wind is stable.

We will attempt here to show that small-scale disturbances of the azimuthal motion propagate with the predicted characteristic velocity, and that their amplitude cannot grow infinitely large. In the treatment of this problem we assume that the radial motion is not affected by disturbances in the azimuthal velocity and magnetic field. Thus u, ρ, and T are functions of r only, whereas v_φ and B_φ are functions of r and time t. The time-dependent azimuthal equation of motion is

$$\left(\frac{\partial}{\partial t} + u\,\frac{\partial}{\partial r}\right)(rv_\varphi) = \frac{B_r}{4\pi\rho}\,\frac{\partial}{\partial r}\,(rB_\varphi) \qquad \text{(III.6.1)}$$

and from Maxwell's equation we obtain

$$\left(\frac{\partial}{\partial t} + u\,\frac{\partial}{\partial r}\right)(rB_\varphi) = B_r\left(\frac{\partial}{\partial r} - \frac{2}{r}\right)(rv_\varphi) - rB_\varphi\,\frac{du}{dr} \qquad \text{(III.6.2)}$$

This set of time-dependent equations was solved by a numerical method. In Appendix B we indicate how the finite difference equations were

written and the sequence of the calculations. As initial condition for the azimuthal velocity we assumed a Gaussian distribution of the form

$$v_\varphi(r,0) = v_{\varphi 0} \frac{(r - r_p)}{r} e^{-\left[\frac{(r - r_p)}{5 r_\odot}\right]^2} \qquad \text{(III.6.3)}$$

where r_p was taken as 7.5 $r_\odot$. The initial value of B_φ is then given by

$$B_\varphi(r,0) = B_r(v_\varphi(r,0) - \Omega r)/u \qquad \text{(III.6.4)}$$

For the radial solution u(r) we used the solution described in Section III.5.

Since the decoupled time-dependent equations (III.6.1) and (III.6.2) are linear in v_φ and B_φ the values of v_φ and B_φ as given above can be considered as disturbances superimposed on the steady-state solution or as arbitrary initial conditions. The only steady-state solution which is physically possible is the one given by Eqs. (III.2.8) and (III.2.9) and thus we expect this initial distribution to spread out and to decrease in amplitude. Since we have decoupled the radial from the azimuthal motion, all disturbances should be propagated through the medium with velocities $u + v_{AN}$ and $u - v_{AN}$, where $v_{AN} = B_r/\sqrt{4\pi\rho}$. This is indeed the case as can be seen from Figure III.6.1. This figure shows the position of points of maximum and minimum amplitudes of the azimuthal velocity as a function of time and space as obtained from the numerical calculations. The characteristics are clearly recognizable and if we calculate the slopes of these curves, they correspond exactly to the predicted values

Figure III.6.1

The lines indicate the position of points of maximum and minimum amplitude of the azimuthal velocity disturbance as functions of time and space. These points were calculated by a computer for the case when the azimuthal equations are decoupled from the radial motion.

FIGURE III.6.1

$u + v_{AN}$ and $u - v_{AN}$. From Figure III.6.1 we can also see that as the main wave component of the disturbance moves away from the region around 7.5 $r_\odot$ the short wave components of the initial disturbances may be observed as they appear there.

Calculations were made for a period corresponding to 10 hours. For the first 5 hours, the amplitudes stayed fairly constant. During the period from 5 to 10 hours the amplitudes seemed to grow, mainly those of the short wavelength disturbances. This does not necessarily imply that the azimuthal motion is unstable, and it is more likely that this growth in amplitude is introduced by the use of the finite difference equations or by round-off errors from the computer. If the difference equations are not absolutely stable, the uncoupling of the azimuthal equations from the radial equations will result in the transfer of energy from the radial motion to the azimuthal motion which in turn will result in a growth of the amplitude of the azimuthal wave disturbances. The case of disturbances traveling with the characteristic velocities can be further studied to see if they have amplitudes which will grow infinitely large.

The two equations (III.6.1) and (III.6.2) can be solved for (rv_φ) or (rB_φ). If we use $\ell = rv_\varphi$ then the partial differential equation for ℓ is given by

$$\left(\frac{\partial}{\partial t} + \frac{du}{dr}\right)\left\{\frac{\partial^2}{\partial t^2} - 2u\,\frac{\partial^2}{\partial t \partial r} + (u^2 - v_{AN}^2)\,\frac{\partial^2}{\partial r^2} + \frac{du}{dr}\left(\frac{\partial}{\partial t} + 2u\,\frac{\partial}{\partial r}\right) - \frac{2v_A^2}{r}\left(\frac{3}{r} - 2\frac{\partial}{\partial r}\right)\right\}\ell = u\,\frac{d^2u}{dr^2}\left\{\frac{\partial}{\partial r} + u\,\frac{\partial}{\partial r} - v_{AN}^2\left(\frac{\partial}{\partial r} - \frac{2}{r}\right)\right\}\ell \qquad \text{(III.6.5)}$$

We now assume that the time dependence of the solution is of the form $e^{-i\omega t}$, where ω is the frequency of the wave. From Figure III.6.1 we can see that $\omega \sim 10^{-3}$ and the results of the previous section indicate that $u/r \sim 10^{-5}$. Therefore $r\omega/u \gg 1$ and thus the changes in the radial velocity occur on a much larger scale than the changes associated with the wave motion. We will now write

$$\ell = A_1 e^{-i[\omega t - \psi_+(r)]} e^{-\alpha_+(r)} + A_2 e^{-i[\omega t - \psi_-(r)]} e^{-\alpha_-(r)} \tag{III.6.6}$$

where the function $\psi(r)$ is defined by

$$\frac{d\psi_\pm}{dr} = \frac{\omega}{u \pm v_{AN}} \tag{III.6.7}$$

and the α's have to be determined. Substituting this expression for ℓ back into Eq. (III.6.5) and defining

$$\beta_\pm = \frac{d\alpha_\pm}{dr} \tag{III.6.8}$$

we find that

$$\beta_\pm = \frac{1}{2(u \pm v_{AN})}\left[\frac{u \mp v_{AN}}{2u}\,\frac{du}{dr} - \frac{u \pm 3v_{AN}}{r}\right] \tag{III.6.9}$$

Now both β_+ and β_- may increase or decrease as r changes, but neither one of the two behaves anywhere in such a way that $e^{-\alpha_\pm}$ increases without bound. For the particular case when $u \approx v_{AN}$ it can also be shown that the solution is perfectly well-behaved near $r = r_a$.

For large r, $v_{AN} \ll u$, $du/dr \ll \frac{u}{r}$ and

$$\beta_\pm \simeq \frac{1}{2u}\left\{\frac{1}{2}\,\frac{du}{dr} - \frac{u}{r}\right\} \simeq -\frac{1}{2r} \tag{III.6.10}$$

i.e.,

$$v_\varphi \sim r^{-1/2}$$

This means that wave disturbances traveling with the characteristic velocity do not have amplitudes which become infinitely large. And thus for this type of disturbances the model presented here is stable.

IV. *THE EFFECT OF VISCOSITY AND ANISOTROPY IN THE PRESSURE ON THE* AZIMUTHAL MOTION OF THE SOLAR WIND

IV.1 General Discussion

From the results obtained in the previous section we can see that for the sun the azimuthal motion and magnetic forces have only a small effect on the radial motion. Even if the azimuthal velocity should increase to 20 km sec^{-1} at 1 a.u., the centrifugal force term will only be of the order of 5% of the acceleration term in the radial equation of motion. Therefore we now assume that a solution of the radial motion is known everywhere and that this solution is not greatly affected by the azimuthal motion or the presence of the magnetic fields. This will permit us to solve the azimuthal equation of motion (II.2.13) as soon as we know or have determined the constant K and the $r\varphi$ component of the stress tensor, i.e., $T_{r\varphi}$.

IV.2 Determination of the Stress Tensor

Results of recent measurements of solar wind properties on Pioneer 6 as reported by Wolf, Silva, McKibbin and Mason (1966) and on the Vela series of satellites (Hundhausen et al., 1967) indicate that $p_{\parallel}$, the pressure in a direction parallel to the interplanetary magnetic field vector, is larger than $p_{\perp}$, the pressure perpendicular to the field. One possibility for this anisotropy is that it is due to the partial conservation of the first adiabatic invariant. The magnetic moment μ is given by

$$\mu = \frac{W_{\perp}}{B} \propto \frac{T_{\perp}}{B} \qquad \text{(IV.2.1)}$$

where the temperature $T_\perp$ is defined by

$$T_\perp = \frac{m}{2k\rho} p_\perp \qquad \text{(IV.2.2)}$$

If μ were to remain constant, then the energy $W_\perp$ in the random motion perpendicular to the field has to decrease as B decreases. B falls off inversely proportional to r^2 in the vicinity of the sun and inversely proportional to r farther out. Thus $T_\perp$ would have to decrease as B. On the other hand the parallel temperature $T_\parallel$, defined in a manner analogous to $T_\perp$ decreases less rapidly than 1/r in the region between the sun and 1 a.u.. This would result in a decrease in $T_\perp$ relative to $T_\parallel$. If the magnetic moment would be totally conserved, $T_\parallel$ should be approximately 25 times larger than $T_\perp$ at 1 a.u. Scarf, Wolfe and Silva (1967) have pointed out that such large anisotropies cannot exist in the solar wind because they cause instabilities, which in turn would then create irregularities in the magnetic fields, turbulence and possible shock waves. These processes would tend to restore the plasma of the solar wind to a more nearly isotropic distribution. This seems to be confirmed by the latest measurements on space probes. Experimental data indicate that $T_\parallel \simeq 2T_\perp$ at the orbit of earth, indicating that the magnetic moment is only very weakly conserved. In a local cartesian coordinate system aligned with its x-axis along the direction of the magnetic field, the pressure tensor may be written as

$$p_{ij} = \underset{\approx}{p} = \begin{pmatrix} p_\parallel & 0 & 0 \\ 0 & p_\perp & 0 \\ 0 & 0 & p_\perp \end{pmatrix} \qquad \text{(IV.2.3)}$$

The off-diagonal terms may in general be different from zero, but they will be smaller than the diagonal terms by a factor of $1/\omega\tau$, where ω is the cyclotron frequency and τ the time between collisions (Simon and Thompson, 1965). In the case of the solar plasma $\omega\tau$ is much larger than unity and thus these off-diagonal terms can be neglected.

From this pressure tensor the hydrostatic pressure is defined by

$$p = \frac{1}{3} (p_{\parallel} + 2p_{\perp}) \qquad \text{(IV.2.4)}$$

and the temperature T of the gas is in turn given by the ideal gas law, Eq. (II.2.18), i.e.,

$$T = \frac{m}{2k\rho} p$$

Under a rotation of the coordinate system through an angle ψ, the local hose angle, the $r\varphi$ component of the pressure tensor is given by

$$p_{r\varphi} = \cos \psi \sin \psi (p_{\perp} - p_{\parallel}) \qquad \text{(IV.2.5)}$$

Since the exact form of $(p_{\perp} - p_{\parallel})$ is not known at the present time, we will assume for convenience that

$$p_{\parallel} - p_{\perp} = \epsilon \sin^2\psi \, p_{\parallel} = \epsilon \frac{B_{\varphi}^2}{B^2} p_{\parallel} \qquad \text{(IV.2.6)}$$

If ϵ is equal to zero we will have a model in which there will be no anisotropy in the pressure. If we set ϵ equal to unity (which will be done for the numerical calculations) then this assumed function will reproduce those values of the anisotropy in the pressure which seem to be indicated at the present time. This function will approach zero near the surface of the sun where $B_{\varphi} \ll B$ and where the pressure is

isotropic. Near 1 a.u., $p_{\|} - p_{\perp}$ will be close to $p_{\|}/2$ which is the value indicated by the experimental observations of the Vela satellites.

In addition to the torque resulting from the ansiotropy in the pressure there exists a torque on the fluid due to the effect of the fluid viscosity. The viscous stress tensor for an ionized fluid with a magnetic field embedded in it has been given by Chapman and Cowling (1952), Braginski (1959), Herdan and Liley (1959), and Burgers (1958). In Appendix A the viscous stress tensor is expressed in spherical polar coordinates, yielding in particular the $r\varphi$-component

$$\sigma^{o}_{r\varphi} = \frac{2\mu}{(1+\alpha^2)(1+4\alpha^2)} \left\{ \frac{r}{2} \frac{d}{dr}\left(\frac{v_\varphi}{r}\right)\left(1 + 4\alpha^2 + 12\alpha^4 \frac{B_r^2 B_\varphi^2}{B^4}\right) \right.$$

$$\left. + \frac{2\alpha^4 B_r B_\varphi}{B^4}(2B_r^2 - B_\varphi^2)\, r \frac{d}{dr}\left(\frac{u}{r}\right) + \frac{2\alpha^2 B_r B_\varphi}{B^2} r \frac{d}{dr}\left(\frac{u}{r}\right) \right\} \quad \text{(IV.2.7)}$$

where $\alpha = \frac{3}{2}\omega\tau$ and μ is the coefficient of viscosity given by Chapman (1954) as

$$\mu = 1.2 \times 10^{-16}\, T^{5/2} \text{ gm cm}^{-1}\text{sec}^{-1} \quad \text{(IV.2.8)}$$

Near 1 a.u. $\omega \simeq 10^{-1}\text{sec}^{-1}$, $\tau \simeq 10^{4}\text{sec}$ and thus $\alpha \simeq 10^{3}$. To the extent that between the sun and 1 a.u. ω is dominated by B_r, it follows from Eqs. (II.2.2) and (II.2.4) that α is proportional to u and hence $\alpha^2 \gg 1$ throughout the entire region where the solar wind has any significance. Thus we can approximate Eq. (IV.2.7) by

$$\sigma^{o}_{r\varphi} = \mu \left\{ 3 \frac{B_\varphi^2 B_r^2}{B^4} r \frac{d}{dr}\left(\frac{v_\varphi}{r}\right) + \frac{B_r B_\varphi}{B^4}(2B_r^2 - B_\varphi^2)\, r \frac{d}{dr}\left(\frac{u}{r}\right) \right\} \quad \text{(IV.2.9)}$$

Except for the factor $3B_\varphi^2 B_r^2/B^4$, the first term on the right-hand side of this equation is the "ordinary" viscous stress. The effect of this stress on the azimuthal motion has been investigated by Pneuman (1966). In his solution very near the sun, v_φ is increased above the solution for $\mu = 0$, but farther out is reduced. This result depends on his particular choice of boundary conditions which, although plausible, we believe to be incorrect. If he had included the factor $3B_r^2 B_\varphi^2/B^4$, which reduces the effective viscous force due to the presence of the magnetic field, this term would become very small and unimportant compared to the other terms near the sun. The second term in Eq. (IV.2.9) is due to the coupling of the radial viscous force to the azimuthal motion. This is caused by the anisotropy of space resulting from the presence of the magnetic field.

IV.3 Solution of the Azimuthal Equations of Motion

With the aid of Eq. (II.2.13) we can write the expression for v_φ in the form

$$v_\varphi = \frac{T_{r\varphi}}{\rho u} + \frac{K}{r} \qquad \text{(IV.3.1)}$$

Equations (II.2.14), (IV.2.5) and (IV.2.8) provide us with explicit expressions for $T_{r\varphi}$ which when substituted in the above equation give

$$v_\varphi = \frac{B_r B_\varphi}{4\pi\rho u} + \frac{\mu}{\rho u}\left\{\frac{3B_\varphi^2 B_r^2}{B^4} r \frac{d}{dr}\left(\frac{v_\varphi}{r}\right) + \frac{B_\varphi B_r}{B^4}(2B_r^2 - B_\varphi^2) r \frac{d}{dr}\left(\frac{u}{r}\right)\right\} - \frac{1}{\rho u}\frac{B_\varphi^3 B_r}{B^4} p_\parallel + \frac{K}{r} \qquad \text{(IV.3.2)}$$

Here ϵ from Eq. (IV.2.5) has been set equal to unity. If the expression

for B_φ as a function of v_φ, u and r given by Eq. (II.2.7) is substituted, the following first order non-linear differential equation for v_φ is obtained after some algebra:

$$v_\varphi^5(1 - M_A^{-2}) + v_\varphi^4\left[\Omega r M_A^{-2} - \frac{K}{r} - 4(1 - M_A^{-2})\Omega r\right] +$$

$$v_\varphi^3\left[2(1 - M_A^{-2})(3\Omega^2 r^2 + u^2) - 4(\Omega r M_A^{-2} - \frac{K}{r})\Omega r + \frac{2kT_\parallel}{m} + \frac{\mu}{\rho} r \frac{d}{dr}\left(\frac{u}{r}\right)\right] +$$

$$v_\varphi^2\left\{2(3\Omega^2 r^2 + u^2)(\Omega r M_A^{-2} - \frac{K}{r}) - 4(1 - M_A^{-2})(\Omega^2 r^2 + u^2)\Omega r - 3\Omega r\left[\frac{2kT_\parallel}{m} + \frac{\mu}{\rho} r \frac{d}{dr}\left(\frac{u}{r}\right)\right]\right\} +$$

$$v_\varphi\left\{(1 - M_A^{-2})(\Omega^2 r^2 + u^2)^2 - 4(\Omega^2 r^2 + u^2)(\Omega r M_A^{-2} - \frac{K}{r})\Omega r + 3\Omega^2 r^2\left[\frac{2kT_\parallel}{m} + \frac{\mu}{\rho} r \frac{d}{dr}\left(\frac{u}{r}\right)\right] - 2\mu \frac{u^2}{\rho} r \frac{d}{dr}\left(\frac{u}{r}\right)\right\} +$$

$$(u^2 + \Omega^2 r^2)^2(\Omega r M_A^{-2} - \frac{K}{r}) + (2u^2 - \Omega^2 r^2)\frac{\mu}{\rho} r \frac{d}{dr}\left(\frac{u}{r}\right)\Omega r - \frac{2kT_\parallel}{m}\Omega^3 r^3 -$$

$$3(v_\varphi - \Omega r)^2 u^2 \frac{\mu}{\rho} r \frac{d}{dr}\left(\frac{v_\varphi}{r}\right) = 0 \qquad \text{(IV.3.3)}$$

This is a first order differential equation and its solution contains one constant of integration in addition to K, both of which must be determined from boundary, continuity or stability conditions. One of the boundary conditions is that for large r when μ goes to zero, rv_φ approaches a constant value. The evaluation of the other constant is much more difficult. To evaluate this second constant of integration, Pneuman (1966) used the condition that $v_\varphi(r_\odot) = \Omega r_\odot$. This implies immediately from Eq. (II.2.7) that $B_\varphi(r_\odot) = 0$. Referring back to

Eq. (IV.3.2) we can see that this would fix the value of $K = \Omega r_\odot^2$, a very much smaller value than that obtained in Section III for the non-viscous case. This value of K clearly does not represent a physical solution and indeed when this value was used in the numerical integration of the equation no satisfying result was obtained. Since the boundary conditions at the sun are not known there is actually no way to determine this constant of integration exactly. On the other hand we can obtain a good approximation of the value of K in the following way. If we estimate the size of the various terms which appear in Eq. (IV.3.3) we find that the term proportional to $\frac{d}{dr}\left(\frac{v_\varphi}{r}\right)$ is much smaller than the other terms in the equation and thus as a first approximation we may neglect this term. The remaining equation is now a fifth-order polynominal in v_φ and depending on the value of K we obtain a particular value of v_φ. The property of this family of solutions is that for all values of K but one, the values for v_φ which one obtains are discontinuous. There exists only one particular solution which passes from a value of $v_\varphi(r_\odot) \sim \Omega r_\odot$ to a value of v_φ which goes to zero as r becomes very large continuously and the value of K associated with this solution is then taken as the constant of integration. This solution for v_φ in the region between the sun and the Alfvénic critical radius is not altered significantly if we restore the first derivative term into the equation.

In order to obtain quantitative results we require a solution to the radial equation of motion. The general behavior of the solution for v_φ can be explored using any reasonable radial solution, although

the detailed behavior of the solution will depend on the particular radial solution used. Thus the particular v_φ obtained from our numerical calculations and presented here should be considered as illustrating the general and not necessarily the detailed properties of the solution.

The particular radial solution which we have used for the calculations presented here was the one obtained from the polytrope model presented in Sections III.2 to III.4. We have also used the solution of the radial equation obtained from a model with heat conduction as discussed in Section III.5 and have found that both solutions for v_φ have a very similar behavior.

The solution to Eq. (IV.3.3) with the coefficients evaluated using the radial solution from the polytrope model yields a value for the constant K of 5.72×10^{18} $cm^2 sec^{-1}$. This implies that the total torque on the sun is slightly less than in the case of the non-viscous model.

Figure IV.3.1 shows the values thus obtained for $v_\varphi/\Omega r$ as a function of radius for the viscous ansiotropic model (curve V) as well as for the non-viscous isotropic model (curve N). The viscous model predicts at the orbit of Earth an azimuthal wind velocity of 5.1 km sec^{-1}, which is approximately 5 times larger than the value obtained from the non-viscous model. This increase in v_φ is completely due to the torque on the outer surface and thus if μ goes to zero, v_φ will drop rapidly. The coefficient of viscosity used here was based on the fact that collisions in the plasma are only due to Coulomb interactions.

Figure IV.3.1

The dimensionless angular velocity $v_\varphi/(\Omega r)$. Curves N and V refer to the solution of the non-viscous, isotropic pressure and viscous, anisotropic pressure models, respectively.

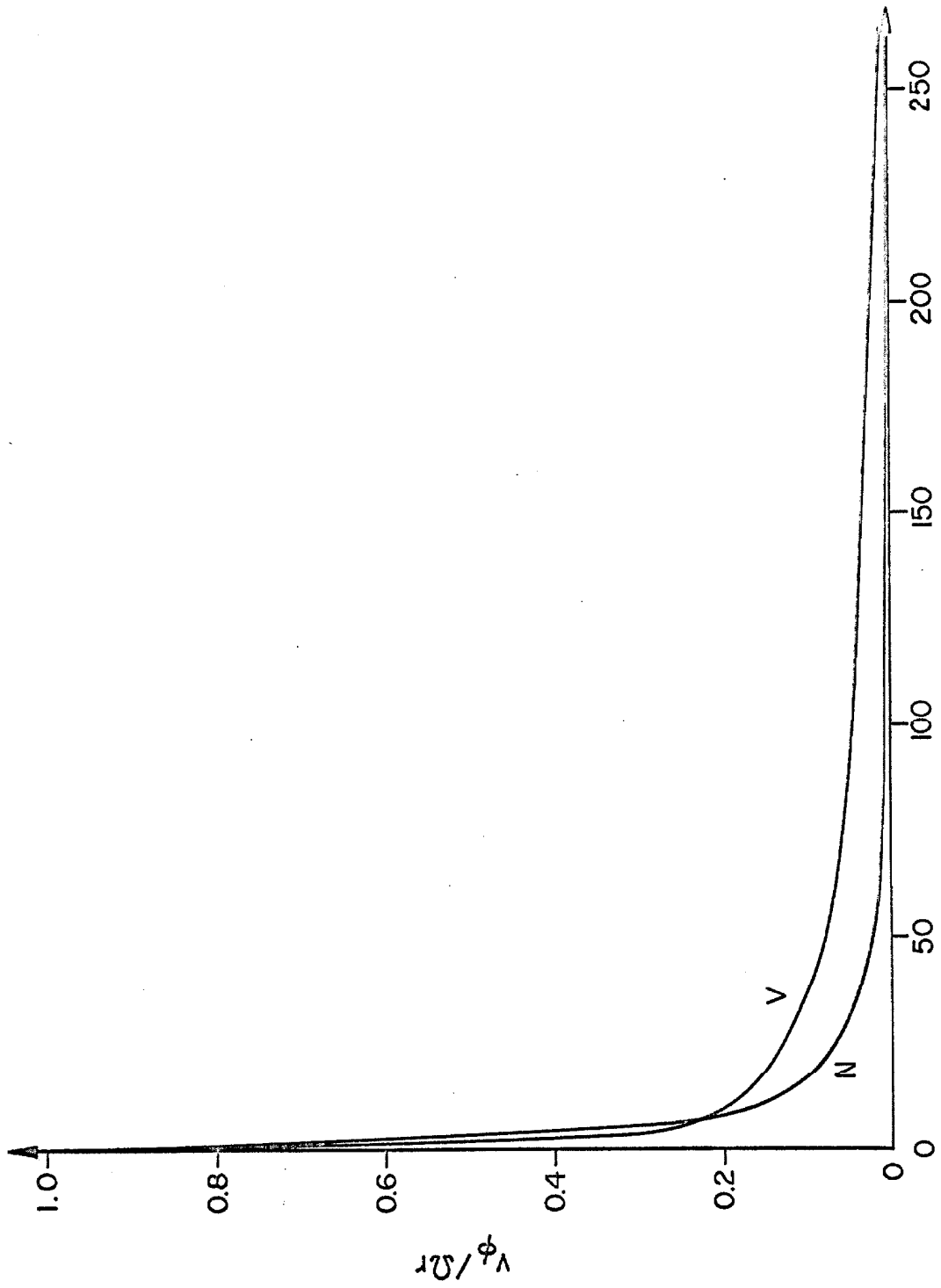

FIGURE IV.3.1

Since we expect other randomizing processes to occur in the gas, the effective value of μ will be much smaller and the effect of viscosity may be completely negligible. The value for v_φ obtained in this section should thus be regarded as an upper limit with the actual value of v_φ being much closer 1 km sec^{-1} at 1 a.u.

Preliminary results from solar wind measurements on Vela 2 by Hundhausen, et al. (1966) indicate an average angle between the solar wind velocity vector and the radius vector of approximately 1.5°, with a variation in direction of approximately 15°. This should be compared with angles of 0.75° and 0.15° predicted by the viscous and non-viscous models, respectively. Thus the theoretical models predict a lower value for the steady-state wind velocity than has been observed on Vela 2. But it should be noted that "the most interesting general feature of the solar wind as revealed by the Vela 2 observations is its non-radial, non-uniform and non-steady nature", (Hundhausen et al., 1966). Thus the averages of the solar wind properties as measured by satellites do not necessarily represent the properties of a steady-state quiet solar wind. We feel that the question of the correct value, even of the correct order of magnitude value of the azimuthal quiet solar wind velocity has not yet been definitely determined from the observations. There exists, of course, the possibility that the azimuthal velocity is substantially increased by disturbances in the solar wind properties and by variations in the interplanetary wind and that in reality no steady-state, quiet azimuthal velocity occurs. If it does occur at times, the theory predicts that the angle between the radius vector and the solar wind velocity vector should lie somewhere between 0.15° and 0.75° for conditions which we regard as typical.

V. SUMMARY

The work which we have presented here makes it possible to understand the large-scale properties of the solar wind, especially of its azimuthal motion. From the analysis of a non-viscous model of the solar wind we have discovered the very important fact, that the azimuthal velocity and the azimuthal magnetic field are determined uniquely by the conditions at the radial Alfvénic critical point r_a. The magnetic field has to arrange itself in such a way that at this critical point the sum of the angular momentum per unit mass plus the torque associated with the magnetic stress has the value $L = \Omega r_a^2$. This condition in turn implies that at the solar surface the magnetic field cannot be purely radial but has to have an azimuthal component. At the surface of the sun the radial velocity of the plasma is very small, but nevertheless finite, and thus the angular velocity of the foot of the lines of force will differ from the angular velocity of the plasma. The size of this differential rotation is governed by the magnitude of the azimuthal magnetic field. Therefore, the conditions at the radial Alfvénic critical point determine the value of the azimuthal magnetic field as well as the value of the angular velocity of the plasma at the surface of the sun and in general throughout space. Even though there is no rigid corotation of the gas with the sun, the gas does convect away a substantial amount of angular momentum and the torque due to the magnetic field is even more effective in decelerating the angular motion of the sun.

Since the location of the radial Alfvénic critical point is important in determining the properties of the angular motion of the solar wind and the torque on the sun, it is useful to estimate the change in r_a caused by reasonable changes in the solar wind parameters as observed near earth. From these parameters M_A can be calculated at 1 a.u., and r_a can then be estimated from the fact that Eq. (III.2.4) shows M_A to be proportional to $u^{1/2}r$. A reasonable approximation, which is a lower limit, is obtained by assuming u to be constant. For example, using our parameter, $M_A = 9.6$ at 1 a.u. and hence $r_a > 22\ r_\odot$, which is a good approximation to the result obtained. Using typical solar wind data, we estimate that the critical Alfvénic radius may lie between 15 $r_\odot$ and 50 $r_\odot$.

The general features of the solution are not changed when we include the effect of viscosity and of an anisotropic pressure in the determination of the azimithal motion. The torques due to both of these forces are very small in the vicinity of the sun and thus the torque on the sun is given essentially in the same manner as for the non-viscous case. The conditions at the sun are again determined by the conditions in the vicinity of the radial Alfvénic critical point and thus viscous forces play a very minor role in decelerating the sun. On the other hand, the azimuthal motion of the gas at distances larger than the critical radius is greatly affected by the torques due to viscosity and anisotropy in the pressure. This torque accelerates the solar wind in the azimuthal direction and we obtain thus at 1 a.u. an angular velocity of the plasma which is substantially higher than for the non-viscous case. But as the viscous forces decrease for large

values of r, we expect the azimuthal velocity to drop rapidly to the value predicted by the non-viscous model. We would also expect a lower angular velocity of the solar wind if the coefficient of viscosity should not be proportional to $T^{5/2}$ as given by Chapman (1954), but should decrease more rapidly with radius. In the solar wind, there exist many processes which may cause a decrease in the viscous forces. Turbulances, shocks and instabilities in the solar wind as well as irregularities in the interplanetary magnetic field all tend to decrease the effective mean free path of the plasma ions and thus decrease the coefficient of viscosity. Since these processes are all transient in nature, we expect to observe large fluctuations in the magnitude of the azimuthal solar wind velocity, which have indeed been observed recently (Hundhausen et al., 1967). The value of v_φ obtained from the viscous model presented here should therefore be considered as an upper limit to the quiet azimuthal solar wind velocity.

During the past year several investigators have discussed topics which were also treated in this report. We wish to mention in particular that the conclusions reached by Modisette (1967) regarding the properties of the azimuthal wind velocity, the azimuthal magnetic field and the torque on the sun are in general agreement with the findings presented here. However, we do not agree with his statement that the large azimuthal solar wind velocity of 9 ± 3 km sec^{-1} at 1 a.u. deduced by Brandt (1966) from observations of type I comet tail deflections can be explained by the "total momentum flux, both in the particles and the fields" causing the deflection. We have already

mentioned in previous sections the model treated by Pneuman (1966). This model possesses a whole family of solutions, from which Pneuman selected a particular one by choosing a specific set of boundary conditions at the sun. We have already commented in Section IV on the validity and the physical significance of his particular choice of boundary values. In view of the findings of this investigation and due to the fact that the boundary conditions at the sun are not known, it is very plausible that the selection of a particular solution will be determined by other criteria which have to be imposed on the behavior of the solution. The azimuthal motion and the magnetic fields do not significantly influence the general behavior of the radial solar wind velocity and thus the actual numerical radial solution obtained from our model is essentially that obtained much earlier by Parker (1963). On the other hand, by including the centrifugal and magnetic force terms in the radial momentum equations, we have altered the basic structure of the radial solution significantly. While in Parker's model all the solar wind properties were determined by the conditions at the sonic critical point r_c, our model requires that the radial solution passes through three critical points in order to satisfy the known boundary conditions, namely that the radial wind velocity at the sun's surface is very small and that the solar wind velocity is supersonic and super-Alfvénic near 1 a.u.. These three critical points are found at points where the radial flow velocity equals the velocity of a characteristic small amplitude wave disturbance in the fluid. And in the presence of magnetic fields we have now three possible modes of

propagation instead of only one as in Parker's model. The existence of these critical points can alter the nature of the radial solution significantly and thus the more complete model presented here has to be used to calculate the properties of stellar winds for stars which have such a high rotation rate or such large magnetic fields that the corresponding terms in the radial equation of motion are important.

Another very important feature of this model is the prediction of two possible branches u_{α_1} and u_{α_2} (see Figure III.3.1) along which the solar wind can expand and still yield a zero pressure at infinity. While both solutions are thus possible we know from observations that the solar wind follows the upper branch u_{α_1} on which its velocity is supersonic and super-Alfvénic. This poses the very interesting question of why the solar wind follows the upper rather than the lower branch. We conjecture that the reason for this is that the conditions along the upper branch are more stable. In passing through the critical points and onto the curve u_{α_2} one encounters a discontinuity in the slope of this curve. If there exists any finite amount of viscosity this discontinuity would be smoothed out, and thus would not cause any trouble. Nevertheless the rather rapid decrease in the radial velocity along the lower branch, and the associated sharp increase in the magnitude of the azimuthal magnetic field and the rapid reversal of the direction of the azimuthal wind velocity seem to indicate that a solar wind expanding along the branch u_{α_2} may be much more susceptible to instabilities than a gas following the upper branch,

along which the gradient of all quantities does not vary significantly over short distances. Furthermore along the lower branch the radial velocity becomes smaller than the local sound velocity and thus disturbances at large distances can propagate upstream. Such a situation is inherently less stable than one in which all disturbances are convected out by the plasma. Thus it is plausible that the conditions are less stable along u_{α_2} than along u_{α_1}, and hence the solar wind expands along the supersonic and super-Alfvénic branch.

As can be seen from the discussion in Section III, the polytrope model is clearly not a model from which we expect an accurate quantitative description of the solar wind over all space. Nevertheless, because of its analytical simplicity, the polytrope model is best suited for a study of the qualitative features of the motion of the solar wind. The general properties of the solution of this particular model and the conclusions we draw from them are equally applicable to the results of more complicated models, which are intended to give better quantitative information on the solar wind, but which may not be as readily understood due to their complexity. The model presented here provides an understanding of the coupling between the magnetic fields and the plasma motion. In particular, from it we have been able to determine the behavior of the angular motion of the solar wind, the shape and value of the interplanetary magnetic field and information on the angular momentum loss of the sun due to its expanding corona.

APPENDIX A

The form of the viscous stress tensor in the presence of a magnetic field has been given by Chapman and Cowling (1952) for the special case when the fluid velocity and the magnetic field are each aligned with one of the axes of a cartesian coordinate system. By a suitable transformation this formula may be expressed in any coordinate system and for arbitrary angles between the velocity and the radius vectors. On the other hand it is much simpler to derive the equations for this case directly. If we define μ to be the classical coefficient of viscosity in an unmagnetized plasma (Chapman, 1954), $\alpha = (3/2)\tau(eB/m)$, where τ is the collision time, e and m are the charge and mass of an ion, respectively, and B is the magnitude of the magnetic field, then Herdan and Liley (1959, 1959) have shown that in a first approximation the symmetrical viscous stress tensor $\underset{\approx}{\sigma}^{\circ}$ may be obtained from the solution of the equation

$$\frac{2\alpha}{B} \ll \underset{\approx}{\sigma}^{\circ} \times \underset{\sim}{B} \gg^{\circ} = -\, 2\mu\, \underset{\approx}{e}^{\circ} + \underset{\approx}{\sigma}^{\circ} \tag{A.1}$$

where $\underset{\approx}{e}^{\circ}$ is the symmetrical traceless velocity gradient tensor and $\underset{\sim}{B}$ is the magnetic field vector. The symmetrized cross product is defined by

$$\ll \underset{\approx}{\sigma}^{\circ} \times \underset{\sim}{B} \gg^{\circ}_{\lambda\mu} = \frac{1}{2}\,\frac{1}{\sqrt{g}} \Big\{ \sigma_{\lambda\epsilon}\, \eta^{\alpha\epsilon\beta} B_{\beta}\, g_{\alpha\mu} + \sigma_{\mu\epsilon}\, \eta^{\alpha\epsilon\beta} B_{\beta}\, g_{\alpha\lambda} - \frac{2}{3}\, g_{\lambda\mu}\, \sigma^{\circ}_{\tau\alpha}\, \eta^{\tau\alpha\beta} B_{\beta} \Big\} \tag{A.2}$$

where $\underset{\approx}{\eta}$ is the completely asymmetrical tensor and g is the determinant of the metric tensor $\underset{\approx}{g}$ given by

$$g_{ij} = \begin{pmatrix} 1 & 0 & 0 \\ 0 & r^2 & 0 \\ 0 & 0 & r^2\sin^2\theta \end{pmatrix} \tag{A.3}$$

The last term on the right-hand side of Eq. (A.2) is identically zero in this particular case since $\overset{\circ}{\underset{\approx}{\sigma}}$ is a symmetrical tensor and $\underset{\approx}{\eta}$ is an asymmetrical tensor. The velocity gradient tensor may be derived as follows. Let us define the covariant velocity vector v_i with components

$$v_i = (v_1, 0, v_3) = (u, 0, r^2\sin^2\theta\,\omega) \tag{A.4}$$

where the local angular velocity ω is assumed to be a function of r only and is defined by

$$\omega = \frac{v_\varphi}{r \sin\theta} \tag{A.5}$$

The velocity gradient tensor $\underset{\approx}{e}$ is obtained by taking the covariant derivative of the velocity vector $\underset{\approx}{v}$ given by the first form of Eq. (A.4), i.e.,

$$e_{ij} = v_{i;j} = \begin{pmatrix} \frac{dv_1}{dr} & 0 & -\frac{v_3}{r} \\ 0 & rv_1 & -\frac{\cos\theta}{\sin\theta} v_3 \\ \frac{\partial v_3}{\partial r} - \frac{v_3}{r} & \frac{\partial v_3}{\partial\theta} - \frac{\cos\theta}{\sin\theta} v_3 & r\sin^2\theta\, v_1 \end{pmatrix} \tag{A.6}$$

The symmetrical traceless velocity gradient tensor $\overset{\circ}{\underset{\approx}{e}}$ is then immediately given by

$$e_{ij}^{\circ} = \frac{1}{2}\left(e_{ij} + e_{ji} - \frac{2}{3} g_{ij}\, e_{\alpha\beta}\, g^{\alpha\beta} \right)$$

$$= \begin{pmatrix} \frac{2}{3}\left(\frac{dv_1}{dr} - \frac{v_1}{r}\right) & 0 & \frac{1}{2}\frac{\partial v_3}{\partial r} - \frac{v_3}{r} \\ 0 & \frac{1}{3}\left(\frac{v_1}{r} - \frac{dv_1}{dr}\right)r^2 & \frac{1}{2}\frac{\partial v_3}{\partial \theta} - \frac{\cos\theta}{\sin\theta} v_3 \\ \frac{1}{2}\frac{\partial v_3}{\partial r} - \frac{v_3}{r} & \frac{1}{2}\frac{\partial v_3}{\partial \theta} - \frac{\cos\theta}{\sin\theta} v_3 & \frac{1}{3}\left(\frac{v_1}{r} - \frac{dv_1}{dr}\right)r^2\sin^2\theta \end{pmatrix} \tag{A.7}$$

But using the second form of Eq. (A.4) the e_{23}^{o} and e_{13}^{o} components reduce to

$$e_{23}^{o} = \frac{1}{2}\{2 \sin\theta \cos\theta\, r^2\omega\} - \cos\theta \sin\theta\, r^2\omega = 0 \tag{A.8}$$

$$e_{13}^{o} = \frac{1}{2}\left\{2r \sin^2\theta\, \omega + r^2\sin^2\theta \frac{d\omega}{dr}\right\} - r \sin^2\theta\, \omega = \frac{1}{2} r^2\sin^2\theta \frac{d\omega}{dr} \tag{A.9}$$

and we have

$$e_{ij}^{o} = \begin{pmatrix} \frac{2}{3}\left(\frac{du}{dr} - \frac{u}{r}\right) & 0 & \frac{1}{2} r^2\sin^2\theta \frac{d\omega}{dr} \\ 0 & \frac{1}{3}\left(\frac{u}{r} - \frac{du}{dr}\right) r^2 & 0 \\ \frac{1}{2} r^2\sin^2\theta \frac{d\omega}{dr} & 0 & \frac{1}{3}\left(\frac{u}{r} - \frac{du}{dr}\right) r^2\sin^2\theta \end{pmatrix} \tag{A.10}$$

The components of the covariant magnetic field vector B_i are given by

$$B_i = (B_1, 0, B_3) = (B_r, 0, B_\phi r \sin\theta) \tag{A.11}$$

Equation (A.1) may now be expanded to give the following six relations:

$$
\begin{aligned}
\sigma_{11}^{o} &= 2\mu\, e_{11}^{o} + 2\alpha \frac{g_{11}}{\sqrt{g}}\, \sigma_{12}^{o} \frac{B_3}{B} \\
\sigma_{22}^{o} &= 2\mu\, e_{22}^{o} + 2\alpha \frac{g_{22}}{\sqrt{g}} \left\{ \sigma_{23}^{o} \frac{B_1}{B} - \sigma_{12}^{o} \frac{B_3}{B} \right\} \\
\sigma_{33}^{o} &= 2\mu\, e_{33}^{o} - 2\alpha \frac{g_{33}}{\sqrt{g}}\, \sigma_{23}^{o} \frac{B_1}{B} \\
\sigma_{12}^{o} &= 2\mu\, e_{12}^{o} + \alpha \left\{ \frac{g_{22}}{\sqrt{g}} \left(\sigma_{13}^{o} \frac{B_1}{B} - \sigma_{11}^{o} \frac{B_3}{B} \right) + \frac{g_{11}}{\sqrt{g}}\, \sigma_{22}^{o} \frac{B_3}{B} \right\} \\
\sigma_{23}^{o} &= 2\mu\, e_{23}^{o} + \alpha \left\{ \frac{g_{22}}{\sqrt{g}} \left(\sigma_{33}^{o} \frac{B_1}{B} - \sigma_{13}^{o} \frac{B_1}{B} \right) - \frac{g_{33}}{\sqrt{g}}\, \sigma_{22}^{o} \frac{B_1}{B} \right\} \\
\sigma_{13}^{o} &= 2\mu\, e_{13}^{o} + \alpha \left\{ \frac{g_{11}}{\sqrt{g}}\, \sigma_{23}^{o} \frac{B_3}{B} - \frac{g_{33}}{\sqrt{g}} \frac{B_1}{B}\, \sigma_{12}^{o} \right\}
\end{aligned}
\tag{A.12}
$$

For the azimuthal equation of motion we need to know only σ_{13}^{o} and solving for it we obtain

$$
\begin{aligned}
\sigma_{13}^{o} &= \frac{2\mu}{(1+\alpha^2)(1+4\alpha^2)} \left\{ e_{13}^{o} \left(1 + 4\alpha^2 + 12\alpha^4 \frac{B_1^2 B_3^2}{B^4 r^2 \sin^2\theta} \right) + \right. \\
&\left. \frac{6\alpha^4 B_1 B_3}{B^2} \left(e_{11}^{o} \frac{B_1^2}{B^2} + e_{33}^{o} \frac{B_3^2}{B^2 r^4 \sin^4\theta} \right) - e_{22}^{o} \frac{3\alpha^2 B_1 B_3}{r^2 B^2} \right\} \\
&= \frac{2\mu}{(1+\alpha^2)(1+4\alpha^2)} \left\{ e_{13}^{o} \left(1 + 4\alpha^2 + 12\alpha^4 \frac{B_r^2 B_\varphi^2}{B^4} \right) + \frac{6\alpha^4 B_r B_\varphi}{B^2}\, r \sin\theta \right. \\
&\left. \left(e_{11}^{o} \frac{B_r^2}{B^2} + e_{23}^{o} \frac{B_\varphi^2}{B^2 r^2 \sin^2\theta} \right) - e_{22}^{o} \frac{3\alpha^2 B_r B_\varphi}{rB^2} \sin\theta \right\} \\
&= \frac{2\mu\, r \sin\theta}{(1+\alpha^2)(1+4\alpha^2)} \left\{ \frac{1}{2} r \sin\theta \frac{d\omega}{dr} \left(1 + 4\alpha^2 + 12\alpha^4 \frac{B_r^2 B_\varphi^2}{B^4} \right) + \right.
\end{aligned}
$$

$$\frac{2\alpha^4 B_r B_\varphi}{B^4}(2B_r^2 - B_\varphi^2)\left(\frac{du}{dr} - \frac{u}{r}\right) + \frac{\alpha^2 B_r B_\varphi}{B^2}\left(\frac{du}{dr} - \frac{u}{r}\right)\Bigg\} \qquad (A.13)$$

To obtain the physical $\sigma^o_{r\varphi}$ component we divide σ^o_{13} by r sin θ, thus

$$\sigma^o_{r\varphi} = \frac{2\mu}{(1+\alpha^2)(1+4\alpha^2)}\Bigg\{\frac{1}{2} r \frac{d}{dr}\left(\frac{v_\varphi}{r}\right)\left(1 + 4\alpha^2 + 12\alpha^4 \frac{B_r^2 B_\varphi^2}{B^4}\right)$$

$$+ \frac{2\alpha^4 B_r B_\varphi}{B^4}(2B_r^2 - B_\varphi^2)\, r \frac{d}{dr}\left(\frac{u}{r}\right) + \frac{\alpha^2 B_\varphi B_r}{B^2} r \frac{d}{dr}\left(\frac{u}{r}\right)\Bigg\} \qquad (A.14)$$

We can similarly show that

$$\sigma^o_{rr} = \frac{2\mu}{(1+\alpha^2)(1+4\alpha^2)}\Bigg\{e^o_{11}\left[1 + 4\alpha^2 \frac{B_r^2}{B^2}\left(1 + \alpha^2 \frac{B_r^2}{B^2}\right) - \frac{2\alpha^2 B_r^2 B_\varphi^2}{B^4}\right]$$

$$+ e^o_{33} \frac{2\alpha^2 B_\varphi^2}{B^2 r^2 \sin^2\theta}\left[\frac{\alpha^2}{B^2}(2B_r^2 - B_\varphi^2) - 1\right]$$

$$+ e^o_{13} \frac{2\alpha^2 B_r B_\varphi}{B^2 r \sin\theta}\left[1 + \frac{2\alpha^2}{B^2}(2B_r^2 - B_\varphi^2)\right]\Bigg\}$$

$$= \frac{2\mu}{(1+\alpha^2)(1+4\alpha^2)}\Bigg\{\frac{2}{3} r \frac{d}{dr}\left(\frac{u}{r}\right)\left[1 + 4\alpha^2 \frac{B_r^2}{B^2}\left(1 + \alpha^2 \frac{B_r^2}{B^2}\right) - \frac{2\alpha^2 B_r^2 B_\varphi^2}{B^4}\right]$$

$$- \frac{2}{3} r \frac{d}{dr}\left(\frac{u}{r}\right) \frac{\alpha^2 B_\varphi^2}{B^2}\left[\frac{\alpha^2}{B^2}(2B_r^2 - B_\varphi^2) - 1\right]$$

$$+ r \frac{d}{dr}\left(\frac{v_\varphi}{r}\right) \frac{\alpha^2 B_r B_\varphi}{B^2}\left[1 + \frac{2\alpha^2}{B^2}(2B_r^2 - B_\varphi^2)\right]\Bigg\} \qquad (A.15)$$

All other components can be derived in a like manner.

APPENDIX B

The time-dependent differential equations for $v_\varphi(r,t)$ and $B_\varphi(r,t)$ are

$$\left(\frac{\partial}{\partial t} + u\,\frac{\partial}{\partial r}\right)(rv_\varphi) = \frac{B_r}{4\pi\rho u}\; u\,\frac{\partial}{\partial r}\,(rB_\varphi) = \eta\, u\,\frac{\partial}{\partial r}\,(rB_\varphi) \qquad (B.1)$$

and

$$\left(\frac{\partial}{\partial t} + u\,\frac{\partial}{\partial r}\right)(rB_\varphi) = B_r\left(\frac{\partial}{\partial r} - \frac{2}{r}\right)(rv_\varphi) - rB_\varphi\,\frac{du}{dr} \qquad (B.2)$$

where $\eta = B_r/4\pi\rho u$ is a constant. The last equation is more conveniently rewritten as

$$\frac{\partial}{\partial t}\,B_\varphi = -\frac{2B_r}{r}\,v_\varphi - B_\varphi\,\frac{du}{dr} - \frac{(u - \eta\,B_r)}{\eta\,r}\,\frac{\partial}{\partial r}\,(rv_\varphi) - \frac{1}{\eta}\,\frac{\partial}{\partial t}\,v_\varphi \qquad (B.3)$$

Since these equations are too complicated to lend themselves to an analytical solution, we will employ a numerical method to investigate their behavior. To use numerical calculations, the differential equations have to be converted to finite difference equations. Since it is only too easy to use difference equations which are not absolutely stable, the answers which one obtains from a numerical treatment of such difference equations do not necessarily represent the solution of the differential equation which they are intended to approximate. There is as yet no adequate theory or complete criteria with which to treat or to test the stability of any but the most elementary finite difference equations. Therefore we have tried to follow as closely as possible the scheme suggested by Richtmyer (1957).

For this approach we use finite Eulerian difference equations where the functions are calculated at specific points in space and time. Those points form a fixed grid in the r,t plane with a spatial separation Δr and a time difference Δt between neighboring points. The values for Δr and Δt were taken as $r_\odot/4$ and 180 sec, respectively, where $r_\odot = 6.96 \times 10^{10}$ cm. We have thus defined a set of points in this r,t plane given by $r = j\Delta r + r_\odot$, $t = n\Delta t$ $(n,j = 0,1,2,\ldots)$. Let the values obtained from the difference equation for $v_\varphi(j\Delta r + r_\odot, n\Delta t)$ and $B_\varphi(j\Delta r + r_\odot, n\Delta t)$ be denoted by $v_{\varphi j}^{n}$ and $B_{\varphi j}^{n}$, respectively. The values of the function $u(j\Delta r + r_\odot)$, $du/dr(j\Delta r + r_\odot)$ and $B_r(j\Delta r + r_\odot)$ are known exactly and will be denoted by u_j, du/dr_j and B_{rj}. Similarly, we will call $(j\Delta r + r_\odot)$ simply r_j.

The finite difference equations are obtained by essentially the procedure that we approximate all derivatives with respect to r by differences centered at the point where the derivative is desired, i.e., using values at $j + 1$ and $j - 1$ to get $(\partial/\partial r)_j$, while derivatives with respect to time at t are approximated by the difference of quantities referred to times t and $t + \Delta t$.

Following this procedure and using the notation described above, the finite difference equations take the form

$$\frac{v_{\varphi i}^{n+1} - v_{\varphi j}^{n}}{\Delta t} = -\frac{u_j}{2r_j\Delta r}\left\{r_{j+1}(v_{\varphi j+1}^{n} - \eta B_{\varphi j+1}^{n}) - r_{j-1}(v_{\varphi j-1}^{n} - \eta B_{\varphi j-1}^{n})\right\} \tag{B.4}$$

and

$$\frac{B_{\varphi\, j}^{n+1} - B_{\varphi\, j}^{n}}{\Delta t} = -\frac{2B_{r\, j}}{r_j} v_{\varphi\, j}^{n+1} - B_{\varphi\, j}^{n} \left(\frac{du}{dr}\right)_j$$

$$- \frac{(u_j - \eta B_{r\, j})}{2\eta r_j \Delta r} \left(r_{j+1} v_{\varphi\, j+1}^{n+1} - r_{j-1} v_{\varphi\, j-1}^{n+1}\right) - \frac{1}{\Delta t \eta} \left(v_{\varphi\, j}^{n+1} - v_{\varphi\, j}^{n}\right) \tag{B.5}$$

Using a set of initial conditions, in particular the one given in Section III.6, we calculate first all v_φ's at the time $t + \Delta t$ from Eq. (B.4) and then use these advanced values of v_φ to calculate the values of B_φ at the new time from Eq. (B.5). This process is then repeated over and over again. Since we are not able to calculate the values of $v_{\varphi\, 0}^{n}$ and $B_{\varphi\, 0}^{n}$ by this method these values have to be fixed. For our model, we assumed that the surface of the sun acts like a mirror and reflects all disturbances and thus assumed that $v_{\varphi\, 0}^{n} = B_{\varphi\, 0}^{n} = 0$. The values of $v_{\varphi\, j_{max}}^{n}$ and $B_{\varphi\, j_{max}}^{n}$ are calculated by linear extrapolation using the values of the functions at the two previous spatial points. Using this sequence of calculations, the results are then given in a series of tables, each of which shows the spatial variations of v_φ and B_φ for a given time. Initially only the main wave component of the initial gaussian disturbance was apparent, but eventually waves with smaller wavelengths become noticeable. The propagation of the maximas and minimas of these waves could be followed to give the characteristics shown in Figure III.6.1. The amplitude of these wavelets often increased markedly with time, but the analysis of Section III.6 indicates that this is an artifact of the numerical analysis rather than an indication of a serious physical instability.

REFERENCES

Alfvén, H., 1947, M.N., 107, 211.

Allen, C.W., 1963, Astrophysical Quantities, Athlone Press, 161.

Biermann, L., 1948, Zeit. f. Astrophys., 25, 161.

Biermann, L., 1951, Zeit. f. Astrophys., 29, 274.

Birkeland, Kr., 1908, The Norwegian Aurora Polaris Expedition 1902-1903. Vol. 1 On the Cause of Magnetic Storms and the Origin of Terrestrial Magnetism, First Section, H. Ashehoug and Co., Christiania.

_____ 1913, ibid, Second Section.

Blackwell, D.E., and Ingham, M.F., 1961, M.N., 122, 129.

Braginski, S.I., 1958, JETP, 6, 358.

Brandt, J.C., 1966, Ap.J., 144, 1221.

Burgers, J.M., 1958, Technical Report No. BN 124 a,b, University of Maryland.

Carovillano, R.L., and King, J.H., 1966, Ap. J., 145, 426.

Chapman, S., 1918, M.N., 79, 70.

_____ 1919, Proc. Roy. Soc. London(A), 95, 61.

_____ 1954, Ap. J., 120, 151.

Chapman, S., and Ferraro, V.C.A., 1931, Terr. Magn. and Atm. El., 36, 77, 171.

Chapman, S., and Cowling, T.G., 1952, The Mathematical Theory of Non-Uniform Gases, C.U.P.

Dahlberg, E., 1964, Ap. J., 140, 268.

Davis, L. Jr., 1966, The Solar Wind, Edited by Mackin and Neugebauer, Pergamon Press, New York, 147.

Davis, L. Jr., Smith, E.J., Coleman, P.J. Jr., and Sonnett, C.P., 1966, ibid, 35.

de Jager, C., 1959, Handbuch der Physik, 52, 80.

Dessler, A.J., 1967, Reviews of Geophysics, 5, 1.

FitzGerald, G.F., 1892, The Electrician, 30, 48.

_____ 1900, ibid, 46, 287.

Forbush, S.E., 1938, Phys. Rev. 54, 975.

_____ 1938, Terr. Magn. and Atm. El. 43, 203.

Friedrichs, K.O., and Kranzer, H., 1958, Non-Linear Wave Motion, New York University Report, NYO-6486, Part VIII.

Herdan, R., and Liley, B.S., 1959, AEI Research Reports A1004 and A1005.

Hundhausen, A.J., Ashbridge, J.R., Bame, S.J., Gilbert, H.E., and Strong, I.B., 1966, Vela Satellite Observations of Solar Wind Ions, Inter-Union Symposium on Solar-Terrestrial Physics, Belgrade, Yugoslavia.

_____ 1967, JGR, 72, 87.

Kelvin, Lord, 1892, Proc. Roy. Soc. London (A) 52, 300.

Landau, L.D., and Lifshitz, E.M., 1959, Fluid Mechanics, Addison-Wesley Pub. Co., Reading, Massachusetts.

Lodge, O., 1900, The Electrician, 46, 249.

Meyer, F., and Schmidt, H.U., 1966, Mitteit. Astron. Gesellschaft, 21.

Modisette, J.L., 1967, JGR, 72, 1521.

Ness, N.F., Scearce, C.S., and Seek, J.B., 1964, JGR, 69, 3531.

Neugebauer, M., and Snyder, C.W., 1966, JGR, 71, 4469.

Osterbrock, D.E., 1961, Ap. J., 134, 347.

Parker, E.N., 1958, Ap. J., 128, 664.

_____ 1960, Ap. J., 132, 821.

_____ 1963, Interplanetary Dynamical Processes, Interscience Publishers, New York.

_____ 1965, Space Sci. Rev., 4, 666.

_____ 1966, Ap. J., 143, 32.

Pneuman, G.W., 1966, Ap. J., 145, 800.

Pottasch, S.R., 1960, Ap.J., 131, 68.

Richtmyer, R.D., 1957, Difference Methods for Initial-Value Problems, Interscience Publishers, New York, 194.

Scarf, F.L., and Noble, L.M., 1964, A.I.A.A.J., 2, 1158.

Scarf, F.L., and Noble, L.M., 1965, Ap. J., 141, 1479.

Scarf, F.L., Wolfe, J.H., and Silva, R.W., 1967, JGR, 72, 993.

Schwarzschild, M., 1948, Ap.J., 107, 1.

Simon, A., and Thompson, W.B., 1965, General Atomics Report GA-6815.

Spitzer, L., 1956, Physics of Fully Ionized Gases, Interscience Publishers, New York.

Störmer, C., 1955, The Polar Aurora, Oxford Press, London.

Sturrock, P.A., and Hartlet, R.E., 1966, Phys. Rev. Letters, 16, 628.

Van de Hulst, H.C., 1950, Bull. Astron. Inst. Netherlands, 11, 135.

Weber, E.J., and Davis, L. Jr., 1967, Ap.J., 148, 217.

Whang, Y.C., Liu,C.K., and Chang, C.C., 1966, Ap.J., 145, 255.

Wolfe, J.H., Silva, R.W., and Meyers, M.A., 1966, JGR, 71, 1319.

Wolfe, J.H., Silva, R.W., McKibbin, D.D., and Mason, R.H., 1966, JGR, 71, 3329.

Wurm, K., 1943, Mitteilungen Hamb. Sternw., 8, 57.